Two-Lane Highway Work Zone Capacity Model and Control Analysis

Wenbo Zhu

A thesis

submitted in partial fulfillment of the

requirements for the degree of

Master of Science in Civil Engineering

University of Washington

2015

Committee:

Yinhai Wang

Scott Rutherford

Zhibin Li

Program Authorized to Offer Degree:

Department of Civil and Environmental Engineering

I

University of Washington

Abstract

Two-Lane Highway Work Zone Capacity Model and Control Analysis

Wenbo Zhu

Chair of Supervisory Committee:

Dr. Yinhai Wang

Department of Civil and Environmental Engineering

Lane closure is a common practice for two-lane highway work zones. To effectively control the open lane to serve both travel directions, it is necessary to implement a traffic control strategy. Due to lane closure, the roadway capacity will drop significantly. The remaining capacity will depend on work zone configurations, traffic parameters and traffic control strategy.

This study develops a mathematical model calculating capacity and vehicle delay specifically for two-lane highway work zones with pre-timed signal control strategy. A VISSIM simulation model is developed and calibrated using field observed data to validate the mathematical model. After fine tuning the parameters, the mathematical model is able to make reasonably accurate delay estimates for both saturated and under-saturated traffic demands, with mean absolute prediction errors between 1% ~ 3%.

Flagger control is incorporated in the VISSIM simulation model using a gap-out distance method. Field observations are used to validate the model outputs. The study then compared flagger control with fixed time signal control under multiple traffic conditions. Results show that at low traffic demands flagger control performs better than fixed time signal control. For the specific work zone site studied, flagger control is able to achieve approximately 10% ~ 20% lower vehicle delay.

The developed models and simulation results can be applied to optimize two-lane highway lane-closure work zone management by reducing overall user delay while maintaining adequate roadway capacity. The optimized pre-timed signal control plan can reduce the user delay to a similar level as that of the actuated or flagger control method and thus can be used to avoid the human operation cost. Sensitivity analysis shows that traffic operators can increase the roadway capacity by reducing work zone length, increasing vehicle travel speed, and making unbalanced signal allocation based on actual traffic demands.

Table of Contents

Table of Figures

Table of Tables

ACKNOWLEDGEMENTS

graduate study, for introducing me to my new life here. Best wishes to Haixiao, Xi and Ziyuan, who are completing their Master's study, and Matt, Luka, Kris, Xingwei, John, Ruimin, Xianzhe and Summer, who will continue this academic journey with me.

Most importantly, I wish to express my deepest appreciation to my parents. Their persistent care and encouragement always incented me to strive towards my goal. I dedicate this thesis to them and love them from the bottom of my heart.

Chapter 1   Introduction

1.1   Two-lane Highway Work Zones

Two-lane highways play an important role of mobility in the state and county highway systems. With the limited pavement life cycle and the overdue road infrastructure rehabilitation, regular maintenance and reconstruction of existing highways are frequent. When construction work requires one lane to be closed, the remaining lane is used to serve traffic in both directions. Capacity drop and vehicle delay will be caused by the lane closure traffic control method. Oftentimes, two-lane highways are constructed on rural areas, and are not designed to serve heavy traffic. A significant capacity drop may have a great impact on the highway network. In construction practice, capacity should be maintained for both directions and users should not incur extreme delay. Studies on the capacity and delay for the scenarios will provide important guidance for practice work zone activities, in terms of minimizing the total cost and the network impact.

Work Zone Scenarios

Depending on the type of construction projects, two-lane highway work zones can be placed at different locations. Three different work zone types are illustrated in Figure 1-1.

Lane closure work zones (Figure 1-1a) are common work zone types associated with pavement rehabilitation and reconstruction. As one-lane is closed, these work zone scenarios have the greatest impacts on traffic flow. For lane closure work zones, implementation of traffic control method is essential to serve movements in two directions. Most two-lane highway lane-closure work zones apply flaggers or temporary signal systems to control the traffic. Right of way is switched between directions and vehicles must stop or slow down

1

before entering the work zone area. Vehicle delay is generated in the process and roadway capacity drops sharply.

Shoulder work (Figure 1-1b) is also a work zone type usually used for guard rail maintenance, shoulder grading, and vegetation clearing. The traffic impact of these work zones is often caused by vehicles decelerating for traffic signs. As most two-lane highways are not equipped with median barriers, vehicles in the lane next to the working shoulder will drive more close to the median lane markers. This will also affect traffic in the other direction. A bottleneck is created for the two-lane highway traffic flows and cause capacity drop in both directions. For most conditions, shoulder work will not have a significant impact.

Figure 1-1c illustrates the lane shift scenario when shoulder work zones encroach part of the lane. In this scenario lane shifts may be utilized in order to maintain enough lateral safe distance. Traffic signs are usually placed to reduce travel speed and diverge vehicles to the shifted lanes. The traffic impact is similar to shoulder work scenario but usually with greater speed reduction.

a. Lane Closure

b. Shoulder Work
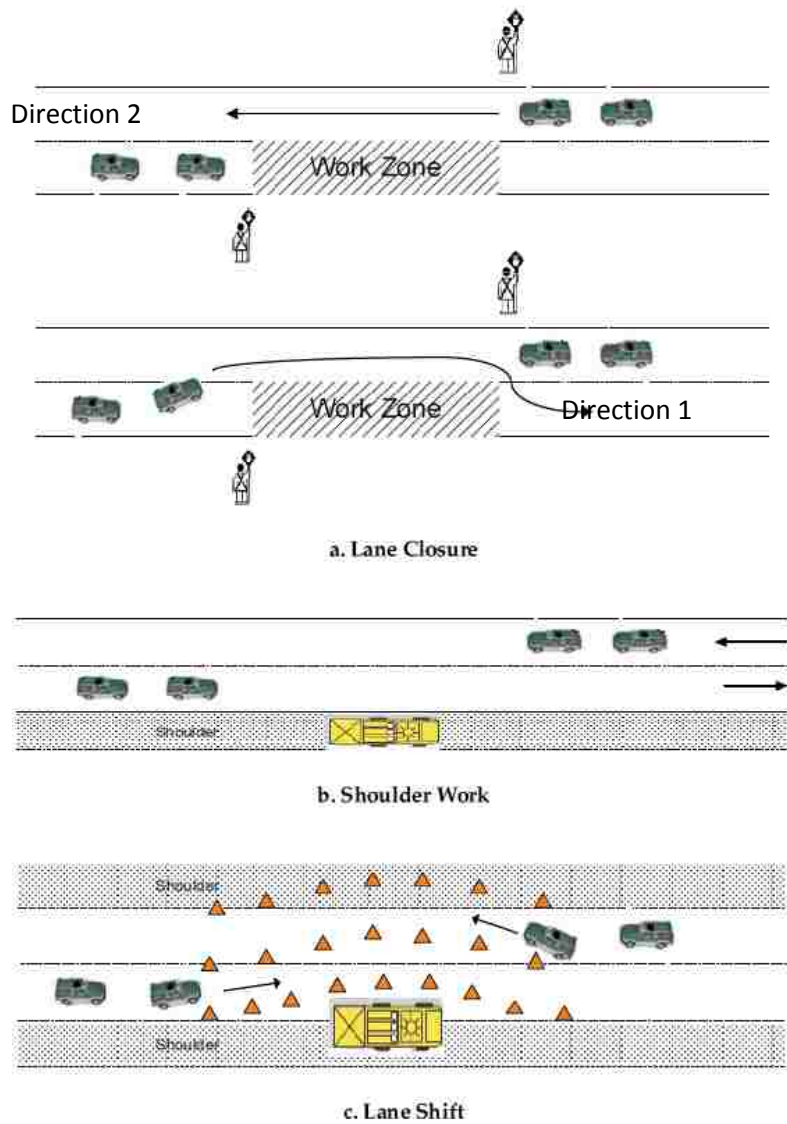
c. Lane Shift

FIGURE 1-1 Two-lane highway work zone scenarios

Compared to shoulder work and lane shift scenarios, lane closure work zones have greater traffic impacts. Movements in two directions are interrupted by the traffic signals/flaggers at both ends of the working area. Estimating the capacity drop and user delay is essential for calculating optimal control settings to serve the on-site traffic and minimize cost. This study focus on the analysis of lane closure work zones on two-lane highways, while we do feel methodologies for other work zone scenarios should also be considered.

1.2   Lane Closure Traffic Control Plans

3

In lane closure work zones, traffic control is needed so that bi-directional traffic flows share the remaining open lane. Oftentimes, flaggers or a temporary signal system would be present to provide alternating right-of-way during the construction period.

Pre-timed Signal Control

Pre-timed signal control requires the implementation of temporary signal heads. Signal timing is pre-defined in the control system. The situation is analogous in certain aspects to a two-phase pre-timed signalized intersection. Each directional traffic flow is restrained when the right of way is given to opposing traffic. Here we define two traffic directions as direction 1 (the travel direction blocked by the work zone) and direction 2 (the travel direction not blocked by the work zone). The two directions are also illustrated in Figure 1-1a. Traffic signals allocate the right-of-way sequentially to vehicles in direction 1 and direction 2.

Just like loss time occurs for intersection traffic signal control, start-up delay and clearance delay are also inevitable. Clearance delay could be particularly large depending on the length and speed limit of the work zone. Vehicle queuing will also be expected in this situation. The length of queue at each side, however, depends on directional travel demands and work zone capacity.

Flagger Control

Flagger control is another commonly used traffic control method on lane closure work zones. Flagging crew equipped with stop and slow signs allocate right-of-way at both ends of the working area. Multiple State DOTs have released flagging manual or training courses for flagging operators, but these documents only provide guidance for performing flagging functions such as stop, slow, and release traffic. No discussion specifically focus on lane

closure work zone control methodology is provided. From our field observation and on-site interview, the flagging operator always releases all the vehicles queued up in his direction and then raises the stop sign to switch the signal for the opposite direction. Due to the length of the work zone, flagging operators at each ends sometimes cannot see each other, and they need to make sure that vehicles in the opposite direction have been stopped before releasing traffic. In this case intercoms are equipped to ensure the communication. But the communication is limited to flagging crew checking the control status of the other side. No specific traffic control interactions between two directions were observed. Because flagger control aims to discharge all vehicles in the queue for each cycle, it is most feasible for short vehicle queues. Thus flagger control is often utilized with low traffic demand and short work zones. For heavy traffic conditions other traffic control facilities such as pilot cars and pre-timed signals are more frequently applied.

Because flagger control is only used for work zones, analysis methodology for signalized intersection control usually do not apply to flagger control. However, as flagging method dynamically changes with real traffic flow, some studies tried to model flagger delay using actuated signal control methods (Cassidy and Son, 1994). This study provided some discussion about the flagging operation nature, and used micro-simulation to model and analyze the flagger control method.

Other Control Plans

Pilot car is another control method often utilized in long-length work zones or moving projects. A pilot car is traveling back and forth in the open lane adjacent to the working area to lead vehicles in two directions. When the opposite traffic is cleared for the work zone area, the pilot car would lead all vehicles queued up to enter the open lane. The traffic impact is similar to flagger control except that vehicle speed when traveling through the open lane is

determined by the pilot car, which is usually slower than free traveling vehicles. For long-length work zones, pilot car control is useful to control vehicle travel speed and thus ensure safety and avoid conflict.

Actuated signals are seldom used in two-lane highway work zones due to the system complexity and requirement of traffic sensors. But actuated signal control is generally a more sustainable dynamic traffic control algorithm than flagger control. For long-term fixed location work zones, actuated signals might be a better solution with lower operation cost.

1.3   Research Objectives

Given the importance of work zone capacity on optimizing construction plans, managing work zones, and reducing agency and user costs, it is imperative to develop analytical procedures or methods for estimating the capacity and delay of work zones. This study aims to provide guidance for two-lane highway lane closure traffic control setting. In developing an optimal traffic control plan, several conditions should be satisfied.

- Direction capacity should be greater than the traffic demand, which means that all vehicles arrived can be served. Vehicle queue will not accumulate in the long term.

- Waiting time or delay incurred by vehicle drivers is tolerable. Delay should be controlled at a reasonable level. It is also associated with controlling user cost.

- Construction and traffic control cost is affordable

- Traffic control facilities are accessible.

Following the conditions listed, the study developed models analyzing capacity and delay for two-lane highway lane closure work zones. An optimal control method is proposed based on minimizing the resultant delay. Two types of traffic control plans, pre-timed signal

control and flagger control, are analyzed and compared. The study will provide instructive

solutions on controlling traffic movements on two-lane highway lane closure work zones.

1.4   Notation of Symbols

Symbols and the corresponding definitions in this paper are summarized in Table 1-1.

TABLE 1-1 Notation of symbols

Symbol	Definition
q	adjusted traffic flow rate (pc/h)
q_i	adjusted traffic flow rate of direction i (i=1 or 2) in the unit of passenger car per second (pc/h)
Q	traffic demand (veh/h)
Q_i	traffic demand of direction i (veh/h)
s_i	adjusted saturation flow rate (queue discharge rate) of direction i (pc/h)
C	cycle length (s)
g_i	effective green time of direction i (s)
$g_{s,i}$	saturated green time of direction i (s)
$g_{i,\min}$	minimum required green signal length of direction i (s)
r	all red time per cycle (s)
l	work zone length (ft)
V_i	average travel speed of direction i (ft/s)
L	total lost time per signal cycle (s)
$t_{s,i}$	start-up lost time in of direction i (s)
$t_{c,i}$	clearance lost time of direction i (s)
c_i	capacity of direction i (pc/h)
c_{total}	total capacity for both directions (pc/h)
$BFFS$	base free-flow speed (mi/h)
SL	speed limit of the two lane highway segment (mi/h)
f_{LS}	adjustment for lane and shoulder width (mi/h)
f_A	adjustment for access-point density (mi/h)
f_{demand}	adjustment for traffic demand in both directions (mi/h)
$f_{np,ATS}$	adjustment factor for the percentage of no-passing zones (mi/h)
f_{HV}	factor for heavy vehicle adjustment (pc/veh)

$\hat{h}_i$	adjusted headway of direction i (s/pc)
h_0	base headway (s/pc)
$f_{speed,i}$	average travel speed adjustment of direction i
d	mean vehicle delay per cycle for both directions (s/veh)
d_i	mean vehicle delay per cycle of direction i (s/veh)
$d_{1,i}$	deterministic delay term in mean vehicle delay (s/veh)
$d_{2,i}$	random delay term in mean vehicle delay (s/veh)
$d_{3,i}$	initial queuing delay per cycle (s/veh)
$d_{o,i}$	mean overflow vehicle delay per cycle of direction i
X_i	volume-to-capacity ratio or degree of saturation of direction i
T	analysis time (h)
m	vehicle arrival adjustment factor
k	controller setting adjustment factor
I	upstream filtering/metering adjustment factor

Chapter 2　Literature Review

Previous studies have limited discussion on two-lane highway lane closure work zones. Considering that a two-lane highway lane-closure work zone section allows only one direction of movement to have the right of way at any given time period, it is very similar to a signalized intersection under two phase control. The analytical process can be developed based on the methodology used for signalized intersections. Traffic guideline documents such as Highway Capacity Manual 2010 (HCM 2010) (TRB, 2010) and Manual on Uniform Traffic Control Devices (MUTCD) (USDOT, 2003) provided detailed methodologies analyzing signalized intersections, including capacity calculation, delay estimation, and signal timing optimization. Study on two-lane highway lane closure work zones mainly focus on developing mathematical model or micro-simulation model to analyze vehicle delay. Some studies did a control plan optimization and proposed suggestion values for optimal work zone length and signal timing.

2.1　Guidance Documents

Capacity Definition

HCM 2010 defines capacity concepts for different traffic modes including vehicle, pedestrian and bicycle. A commonly accepted definition for roadway vehicle capacity is the maximum number of vehicles that can pass a given point during a specified period under prevailing roadway, traffic, and control conditions.

As for work zone capacity, HCM only tackles some configurations of freeway work zones, which are quite different from two-lane highway work zones with one-lane closed. Because lane closure traffic control is similar to intersection signal control, the capacity of two-lane highway lane closure work zones can be derived from intersection capacity

9

Intersection capacity for a lane or a lane group is defined in HCM 2010 as the maximum hourly flow rate that can reasonably be expected to pass through the intersection under prevailing traffic, roadway, and signalization conditions. This capacity is computed as a product of adjusted saturation flow rate and effective-green-to-cycle-length ratio.

Few studies have discussed about the definition for two-lane highway work zone capacity. An example of them is Washburn et al. (2008) conducted by the University of Florida. In the FlagSim simulation tool developed by Washburn et al. (2008), the two-lane highway work zone capacity is determined indirectly through the measured saturation flow rates and proportions of "green" time. This version of capacity definition is concluded from the calculation method.

In this research, from the basic concept of vehicle capacity, we define the *two-lane highway lane-closure work zone capacity* as *the maximum hourly flow rate at which vehicles of both directions can be reasonably expected to pass through the open lane of the work zone area under prevailing traffic, roadway, environmental, and traffic control conditions.*

Clarification of Units

Although capacity is represented by the hourly number of vehicles in the definition, it is calculated in the unit of passenger car per hour (pc/h). For most cases, the unit of passenger car is specifically used for variables in capacity related calculations, such as capacity, saturation flow rate, demand flow rate, etc. In HCM 2010, traffic demand is referred in the unit of vehicle per hour (veh/h), while capacity and traffic flow rate is usually referred in the unit of passenger car per hour (pc/h). Traffic flow rate can be calculated by adjusting traffic demand with the heavy vehicle factor. One heavy vehicle is equivalent to more than one passenger cars. The value of heavy vehicle equivalents depends on vehicle type, traffic

control, roadway grading, etc. The relationship between these two units is expressed in Equation 2-1.

$$q = \frac{Q}{f_{HV}}$$
(2-1)

One major advantage of measuring capacity using passenger car is that it excludes the impact of heavy vehicles. Change in heavy vehicle percentage will not influence the corresponding capacity as long as other variables keep the same. But heavy vehicle ratio will influence the actual number of vehicles can be served. For a typical lane or lane group with certain capacity, an increase in heavy vehicle percentage will result in less actual vehicles that can pass through.

Depending on the specific question addressed, sometimes traffic flow rate is also represented in veh/h in HCM 2010. As passenger car is a unit introduced specifically for capacity analysis, it's not very widely accepted. Most studies does not distinguish between these two units, and units measured by vehicle are more commonly used. In our literature review and study, we do feel that clear distinguishing between these two units should be recognized and considered. In this study capacity is measured in pc/h.

For delay calculation both HCM 2010 and related studies use second per vehicle (s/veh) to measure vehicle delay. As some widely used delay estimation methodologies have been developed based on the unit of second per vehicle, we also use s/veh to measure vehicle delay in this study. Although capacity and delay are not measured in the same unit system, passenger car and vehicle are actually comparable units. More specific discussion about variable units will be introduced in the mathematical model development part.

Capacity Calculation

Intersection capacity is calculated as the product of saturation flow rate and effective green signal ratio. For two-lane highway work zones, as traffic control plan is implemented, directional capacity can be calculated in a similar way.

The procedure recommended by the HCM 2010 for determining the saturation flow rate of a signalized intersection involves counting and timing the number of queue discharge vehicles that passes through an intersection in order to determine the saturated vehicle headway (s/veh). To obtain statistically significant queue discharge vehicle headway values, the average headway is calculated from queue discharge vehicles over 15 control cycles. This headway value is known as the saturation headway and it can be reciprocated to obtain the saturation flow rate. For capacity calculation, the saturation flow rate is adjusted by heavy vehicle factor to obtain the value measured in pc/h.

As the highway work zone signal typically has a much longer cycle length compared to a typical intersection, which usually has a cycle length of approximately 2-3 minutes, we recommend that the time period for computing the capacity be 30 minutes to 1 hour. Of course, a longer time period is generally more desirable when possible. The capacity is determined through the measured saturation flow rate and effective-green-to-cycle-length ratio.

2.2   Vehicle Delay Estimation

Well-developed methodologies for signalized intersection delay prediction has been summarized in previous studies (Akcelic and Rouphail, 1993) (Dion, et al., 2004). Similar to signalized intersections, two-lane highways work zones use traffic control to make the open lane serve for both directions. Vehicles will queue up at signal heads or before traffic operators and wait for signal to travel though the work zone area.

For a typical lane group or direction i, average vehicle delay at traffic signals can be expressed as

$$d_i = d_{1,i} + d_{2,i}$$ (2-2)

The mean vehicle delay is composed of deterministic term and random term. Deterministic vehicle delay can be calculated under the assumption that vehicle arrival rate is uniform. In reality, traffic flow is not perfectly uniform, and number of vehicles arrived for each cycle may vary. Study shows that the randomness feature on traffic flow will have a positive impact on mean vehicle delay at signals. Thus a random delay term is also added to address the variations in vehicle arrival rate.

Deterministic queuing model

Deterministic queuing model can predict vehicle delays assuming uniform traffic flow rate. Two types of traffic conditions, under-saturated flow and over-saturated flow, are considered separately. For under-saturated condition, number of vehicles arrived at signal is less than the number of vehicles the signal can serve. Effective green time is not fully used for queue discharge. Figure 2-1 illustrates the queuing diagram for two sequential signal cycles. The shaded area represents the total delay in each cycle. Mean vehicle delay can be calculated by averaging this among all vehicles arrived during the cycle, which is expressed in Equation (2-3). As traffic flow is uniform, mean vehicle delay does not vary from cycle to cycle.
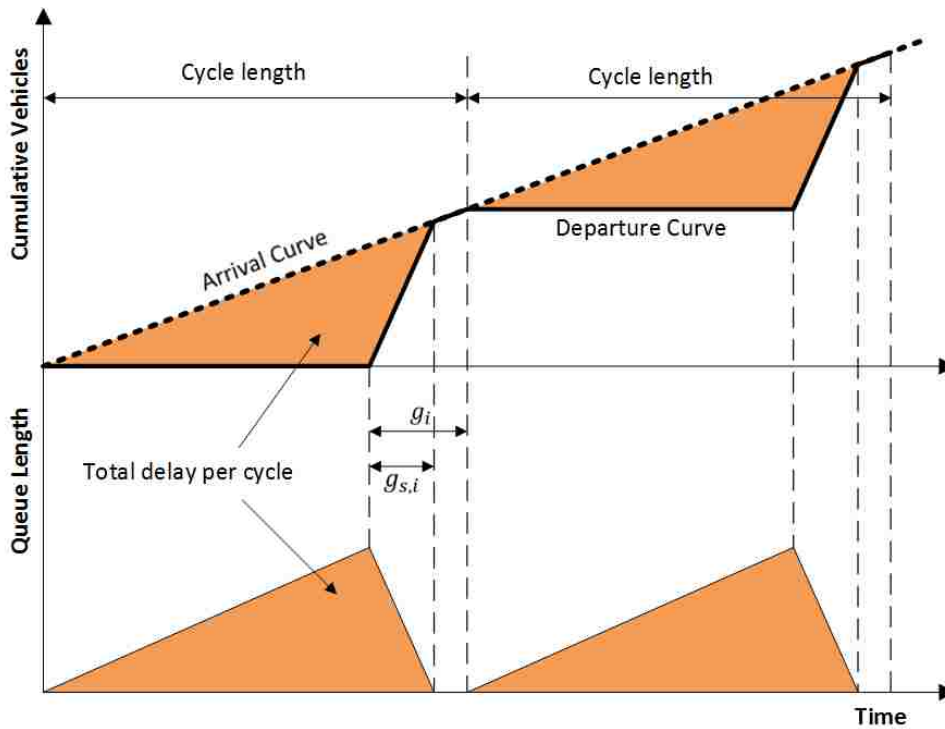
FIGURE 2-1 Deterministic queuing diagram for under-saturated traffic

$$d_{1,i} = \frac{C\left(1 - \dfrac{g_{s,i}}{C}\right)}{2\left(1 - X_i \dfrac{C}{g_{s,i}}\right)}$$

(2-3)

where

$X_i = q_i / c_i$, which is the volume-to-capacity ratio or degree of saturation

The base unit for Equation is second per vehicle (s/veh). Note that in capacity calculation, traffic flow rate and directional capacity are adjusted to the passenger car equivalents. In this equation the unit is normalized when taking the volume-to-capacity ratio, thus the calculated result should still be in the unit of second per vehicles.

The saturated green time, $g_{s,i}$, represents the portion of effective green time used for queue discharge. During this period vehicles leave the signal head at the saturation flow rate, and there are still vehicles waiting in the queue. For saturated traffic conditions, effective green time is totally used for queue discharge, hence equal to the saturated green time. The

14

traffic balance is expressed in Equation (2-4). For under-saturated conditions, saturated green time is shorter than the effective green time, which means that the number of vehicles arrived does not reach the number of vehicles the signal can serve. The traffic balance for under-saturated traffic flow is expressed in Equation (2-5).

$$q_i C = s_i g_i \qquad (2\text{-}4)$$

$$q_i C = s_i g_{s,i} + q_i \left(g_i - g_{s,i} \right) \qquad (2\text{-}5)$$

The left side in Equation (2-5) indicates the number of vehicles arrived at the signal in each cycle, while the right site calculates the number of vehicles left the signal. Vehicles departure can be divided into two time periods, as illustrated in Figure 2-1. Before the queue is fully discharged vehicles will leave the signal at the saturation flow rate. When there is no vehicle queuing up, the departure rate will keep the same as the traffic flow rate.

Over-saturated condition is more complicated. Figure 2-2 illustrates the queuing diagram. Vehicles arrived at the signal exceeds the capacity, and this causes vehicle queue for each cycle cannot be fully discharged. A growing vehicle queue is accumulated before signal heads. As shown in the figure, average vehicle delay is the sum of uniform delay and overflow delay. While uniform delay per cycle can still be predicted using Equation (2-3), overflow delay increases with time. Mean vehicle overflow delay can be predicted by Equation (2-6).
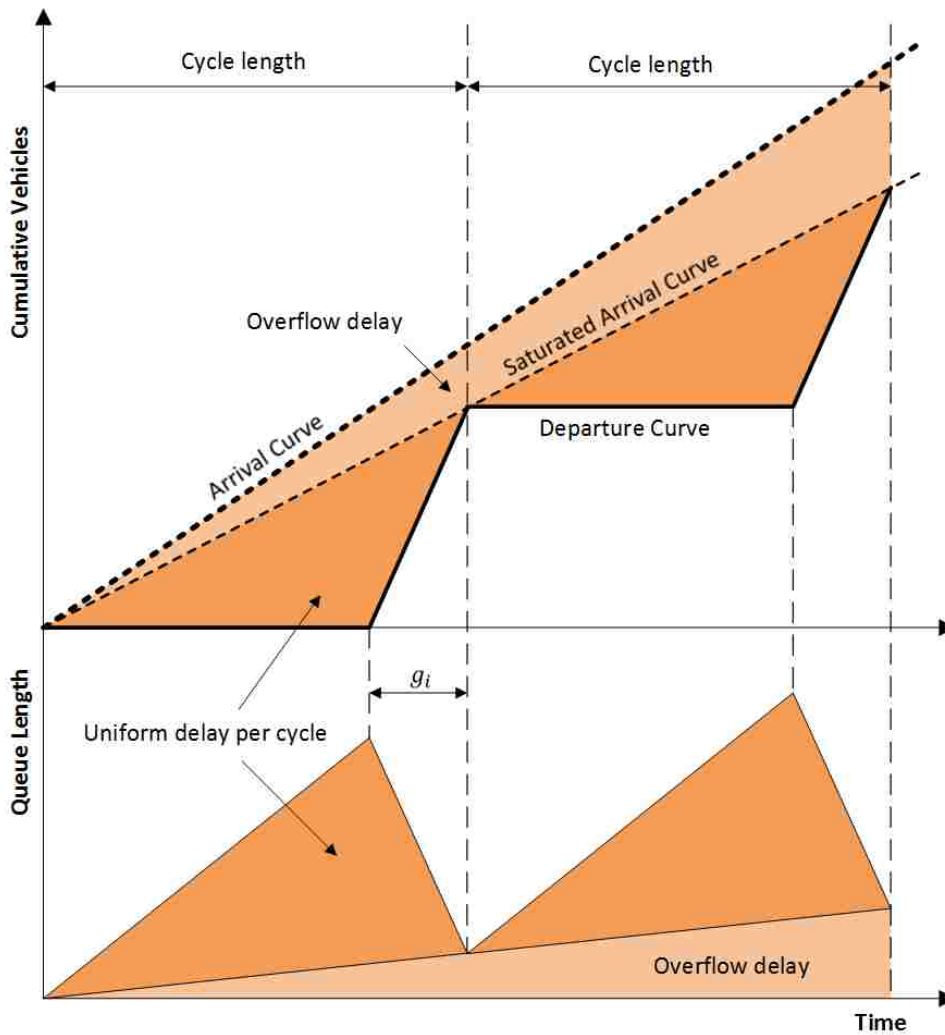
FIGURE 2-2 Deterministic queuing diagram for over-saturated traffic

$$d_{o,i} = \frac{3600T}{2}(X_i - 1) = 900T\left((X_i - 1) + \sqrt{(X_i - 1)^2}\right) \qquad (2\text{-}6)$$

Note that overflow delay only occurs when traffic flow is greater than the capacity. In order to ensure overflow delay equal to 0 when $X_i \leq 1$, $(X_i - 1)$ is transformed to

$(X_i - 1) + \sqrt{(X_i - 1)^2}$. From Equation (2-6) overflow delay is time dependent.

Combine Equations (2-3) and (2-6), a general equation to predict mean vehicle delay for both under-saturated and over-saturated can be expressed as

$$d_{1,i} = \frac{C\left(1 - \dfrac{g_{s,i}}{C}\right)}{2\left(1 - X_i \dfrac{C}{g_{s,i}}\right)} + 900T\left((X_i - 1) + \sqrt{(X_i - 1)^2}\right) \qquad (2\text{-}7)$$

Stochastic Delay Model

While deterministic delay model assumes uniform arrivals, real traffic is not perfectly uniform. Stochastic delay models are developed to address the randomness in vehicle arrival and speed. Study shows that for pre-timed signal control, randomness in traffic flow will cause a positive effect on mean vehicle delay. Thus a random delay term is added to the delay function. For low volume-to-capacity ratios, the random delay should be very small, and for over-saturated traffic, vehicle arrival will approximate uniform distribution, thus impact of randomness is not significant. Values of random delay peaks when *q/c* ratio is around 1.0.

Based on Equation (2-7), a curve showing how deterministic delay changes with volume-to-capacity ratio is illustrated in Figure. A fitted time-dependent model with random delay considered is also included. For low degrees of saturation, actual delay is close to the result of the deterministic queuing delay model. For degrees of saturation greater than 1.0, the model produces delay estimates tangent to the deterministic queuing model of over-saturated conditions.
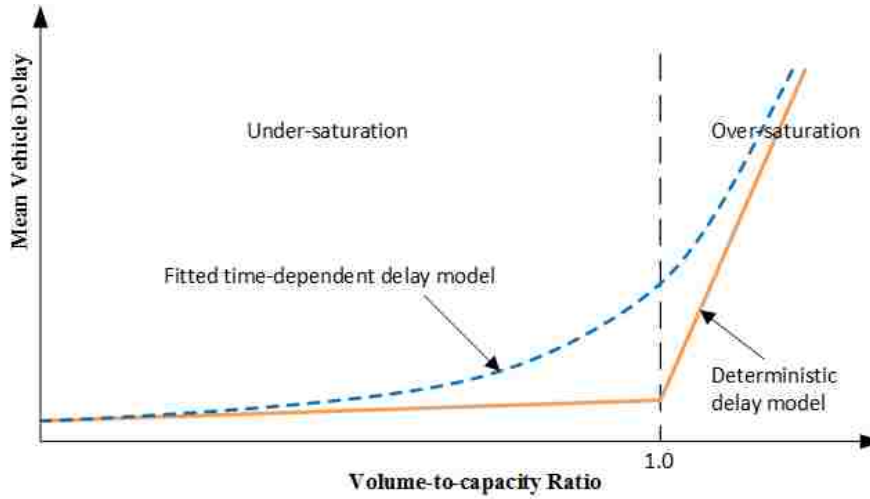
FIGURE 2-3 Delay curve for deterministic model and fitted model

Depending on which approximation method to apply, different forms of stochastic delay models were studied. The model recommended by HCM 2010 is presented in Equation (2-8). The model is proved to yield reasonable delay estimations although it does not base on theoretical derivations.

$$d_{2,i} = 900T\left(\sqrt{(X_i - 1)^2 + \frac{mkI}{cT}X_i} - (X_i - 1) \right)$$
(2-8)

Specific values of model factors have been assigned to the model. For pre-timed control, $k = 0.5$, and if the signal is isolated, $I = 1.0$. For two-lane highway work zone pre-timed signal control, as the traffic signal is isolated from other intersection signals, delay model take these two values. The parameter m accounts for the randomness in vehicle arrivals. Larger m values indicate more random traffic flows. HCM 2010 recommends $m = 8$ for signalized intersections. But two-lane highway work zones usually have lower traffic demand and long clearance time than normal intersections. Randomness in vehicle arrival and travel speed may have different influence on the delay results. For example, vehicles might have a larger speed variation when travelling through the work zone area. Compared to urban intersections, rural two-lane highways usually serve lower traffic demands. Vehicles

18

arrival pattern is also different. Thus in our further discussion, the parameter *m* is modeled by micro-simulation to better address the random delays at lane closure traffic control signals.

Combine Equations (2-7) and (2-8), directional mean vehicle delay can be predicted using Equation (2-9).

$$d_i = \frac{C\left(1 - \frac{g_{s,i}}{C}\right)}{2\left(1 - X_i\frac{C}{g_{s,i}}\right)} + 900T\left((X_i - 1) + \sqrt{(X_i - 1)^2 + \frac{mkI}{cT}X_i}\right) \qquad (2\text{-}9)$$

In the mathematical model development part different values of vehicle arrival adjustment factor are tested and delay predictions are compared to micro-simulation results.

2.3   Delay Modeling and Control Optimization

Due to the stochastic nature of the flagging operation, there are few studies specifically address the delay caused by two-lane highway lane closure traffic control. One of the major piece of analysis done by Cassidy and Son (1994) was to estimate the delays generated by the two-lane highway construction activities. They developed a model on the basis of queuing theory, in which the delays are primarily a function of directional traffic demand, work zone physical length, travel time through work zone and green time. To accommodate the randomness in flagger control, an approximate technique is used in the mathematical model based on actuated signal control. Two types of traffic conditions are considered separately. For under-saturated conditions where the directional queues are completely served during with allocation of right-of-way, the stochastic mathematical model proposed in the study is utilized. For oversaturated conditions, delay is calculated using deterministic queuing theory. Mathematical model predictions were compared with Monte-Carlo simulation results. Average value and variance of traffic flow rate during different time periods were observed to

fit the vehicle arrival distribution in micro-simulation model. The stochastic mathematical model appears to provide reasonable predictions of mean and percentile values of vehicle delay.

Shibuya, et al. (1996) measured traffic flow characteristics at multiple work zone sites and developed a computer simulation program to analyze vehicle delay caused by lane closure control. In the micro-simulation process, average and standard deviation values of arrival headway, departure headway, acceleration, work zone speed and free speed were incorporated as model input. Computer simulation generated reasonable predictions of signal timing and vehicle delay close to field measurements. Then the simulation model was applied to analyze more traffic conditions. The study proposed three methods for estimating flagger control green intervals, by nomograph, regression equation, and analytical optimization. An optimized actuated signal control is recommended as a substitute for flagging operators.

Ceder (2000) developed a theoretical cost model to derive optimal strategies for two-lane highway work zone control. The model considered both user cost incurred by vehicle drivers and operation cost incurred by construction agencies. The optimal work zone length and signal timing is calculated as the model suggests. A sensitivity test revealed that the optimal solution is very sensitive to variables such as fuel price and wage under low traffic demands. For heavy traffic conditions the optimal control strategy is insensitive to these variables.

A similar optimization analysis is done by Schonfeld and Chien (2002). The study developed an optimal strategy, which is determined by work zone length and signal timing, for lane closure work zone operations. Results indicate reducing work zone length is an effective way to increase the control performance and mitigate the user delay, but it will cause increase in maintenance delay.

2.4   Microscopic Simulation Study

More recent studies focus on developing micro-simulation tools for work zone traffic analysis. These studies aims to provide guideline tools for maintenance planners.

An Excel-based software tool to estimate queues and delays in work zones is released by the Federal Highway Administration (FHWA) (Curtis, 2001). The tool could help users quantify the delays and costs of a road construction project. Two-way, one-lane operations modeling is one of the function included in the tool, and the software also has a specific built-in module for flagger control. The 2.0 version of the software improved its function on two-lane highway work zone modeling (12). But the model usability is limited by the difficulty in control specification and lack of analysis procedure. The Colorado DOT also developed a Lane Control Strategy model that can calculate the capacity for a work zone (DeGuzman, et al, 2004).

A more recent simulation tool, FlagSim was developed by Washburn, et al. (2008) to simulate two-lane highway lane-closure work zone traffic flow under flagging operations. Work zone traffic flow data generated by FlagSim was used to develop analytical models to calculate work zone capacity, delay, and queue length. These models were validated using the simulation data generated by Cassidy and Son (1994) for their model development.

2.5   Limitations of Previous Studies

Previous research provides instructive experience for two-lane highway work zone analysis, but some limitations still exist due to the research scope and field data utilized. Most studies developed the delay model based on the signalized intersection methodology. Randomness in flagging control strategy was not discussed and emphasized specifically. Some optimal analysis also lack field data to validate the suggested optimal solutions.

Chapter 3   Study Data

Data for this research is collected as part of the NCHRP 3-107 project tasks. It contains three major subsections: data collection methods, study site selection, and data processing.

First introduced is the data collection needs and methods. In order to investigate impacts of various types of work zone configurations and traffic flow patterns on two-lane highway work zone capacity, both field data and simulation data are needed. Field data will be collected through high-resolution traffic sensors, coupled with surveillance camera recordings. Considering that field data cannot cover the entire spectrum of desired variable ranges, simulation experiments are needed to fill in the data gaps. Simulation data will be generated using VISSIM, a microscopic traffic simulation tool widely used for traffic analysis, in this study.

Field data collection is expensive. Study sites must be carefully selected to best satisfy the research needs under the budget constraints. Site selection criteria and candidate sites are described in the study site selection subsection. Considering that capacity impacts of non-lane closure work zones can be estimated through adjusting existing HCM methods, our data collection efforts will be focused on lane closure scenarios.

The proposed data collection protocol is then described in the data processing subsection. Meeting the needs of capacity, queue length, and delay model development for the lane closure work zones are major considerations in designing the data collection protocol and processing procedures.

After introducing the data collection plan and method, a summary of field collected data will also be presented in this chapter. Simulation data collection will be discussed in more detail in later chapters.

3.1   Data Collection Method

Work zone projects scheduled during the period of the project provide great opportunities for field data collection. However, those projects will not fully cover the types and ranges of the variables to be analyzed in this study. Therefore, both field data and simulation data will be needed for two-lane highway work zone capacity analysis. To fill up gaps in the field data, microscopic simulation experiments will be employed to evaluate the impacts of different traffic flows and flagger control strategies on two-lane highway work-zone capacity. Of course, to trust the simulation results, field data must be used to carefully calibrate and validate the simulation models. Figure 1 illustrates the general relationship between field data and simulation data for simulation experiments. Figure 3-1 illustrates the general relationship between field data and simulation data for simulation experiments.
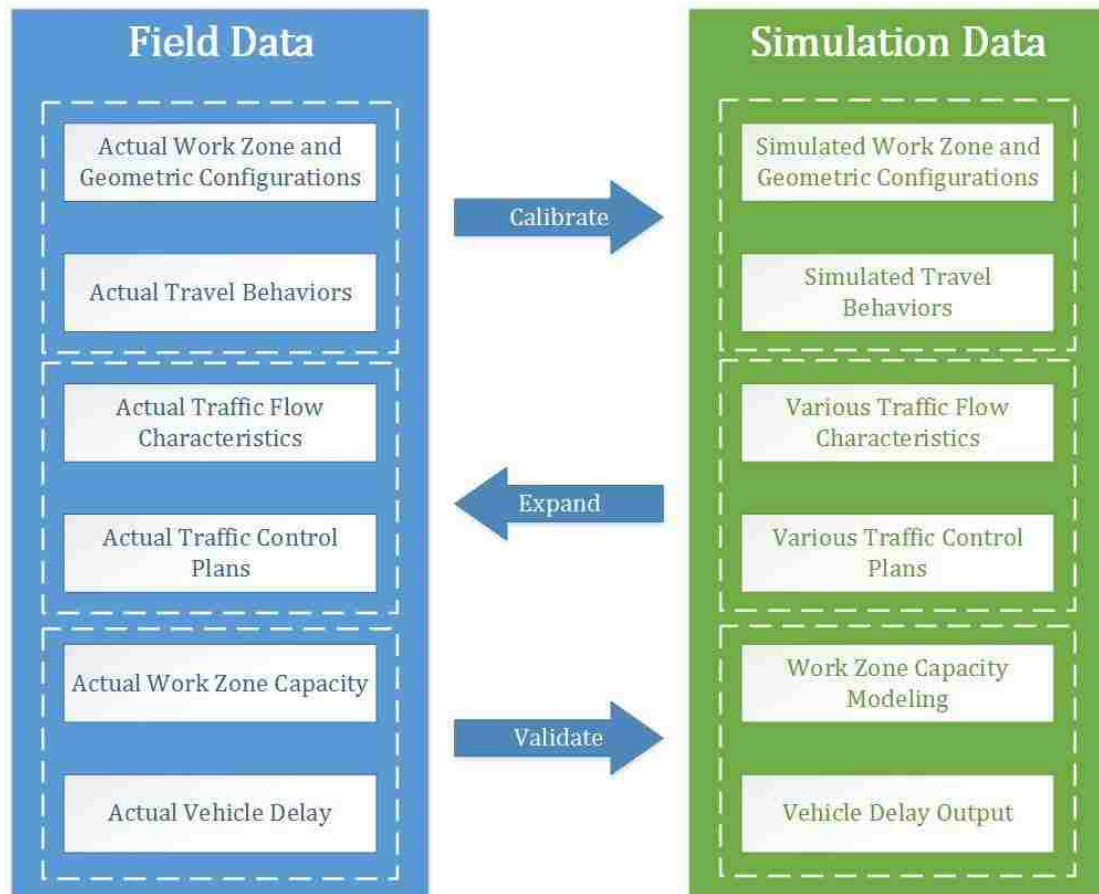
FIGURE 3-1 Relationship between field data and simulation data

The field data of a specific study site will provide basis for the actual work zone configurations, saturation flow rates, traffic control methods, driver behaviors and travel speeds through the work zones, and lane shifting times for vehicles and trucks. It will serve as the ground-truth dataset for simulation model calibration and validation. A well-calibrated microscopic simulation model will help test scenarios with various types of work zone configurations, traffic flow characteristics, and traffic control methods. That is, the simulation experiments will provide simulation outputs for testing the impacts of different traffic control strategies under various demands.

Field Data Collection

The field data includes work zone configurations, roadway geometry, traffic control methods, and traffic flow characteristics. Among them, work zone configuration, roadway geometry, and traffic control methods are manually observed. Traffic flow characteristics information is collected via traffic sensors, e.g. inductive loop detectors, and video cameras. More details of each data variable are listed below.

Work zone configuration

- Work zone location and subject street name

- Work zone duration (working time, e.g. 9:00am - 5:00pm)

- Length of work area

- Lane closure or non-lane closure

- Construction intensity

- Presence (or lack) of raised curb on outside edge of street

Traffic Control Methods

- Flagger or temporary signal control methods

- Posted work zone speed limit

- Posted speed limit for non-work zone area

- Length of shifting area (from work zone edge to stop bar)

Roadway Geometry

- Lane width (provided by WSDOT or measured adjacent to work area)

- Shoulder width for the non-closure lane

- Light and weather condition

- Lateral clearance to work activities

Traffic flow Characteristics

- Traffic demands for blocked lane travel direction and un-blocked lane travel direction

- Truck percentage (including small truck, medium truck and large truck)

- Queue arrival and discharge patterns

- Work zone travel speed

- Lane shifting time

- Start-up lost time

- Traffic throughput, queue length, and delay

Video Data Collection

For most two-lane highway work zone locations, traffic sensors such as loop detectors are unavailable. Thus traffic flow data is collected via video cameras. Figure 3-2 presents a typical layout for video equipment setups.
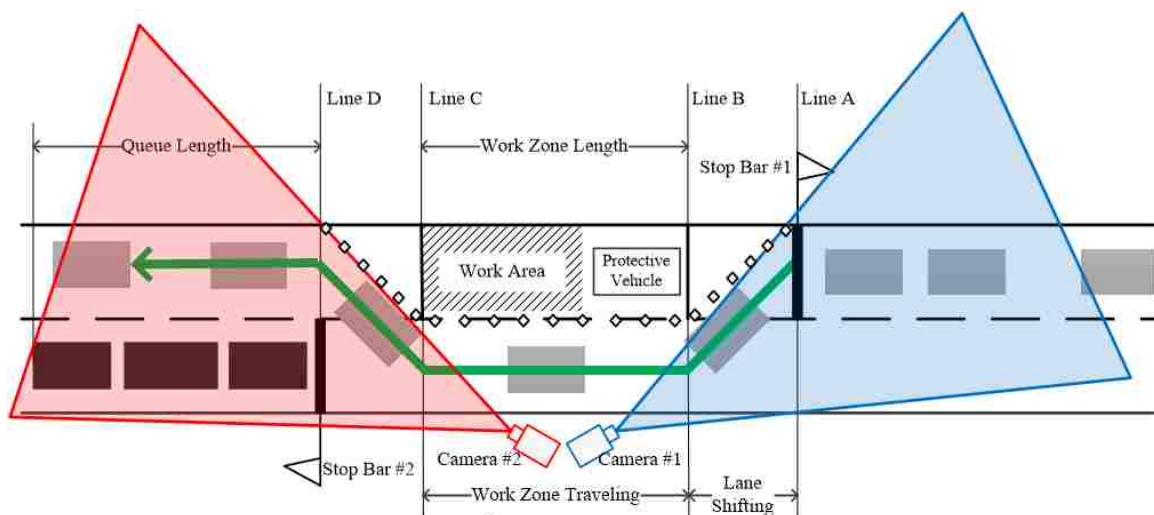
FIGURE 3-2 Traffic data collection using video recording

In this task, two cameras are needed for each work zone to monitor traffic in the close vicinity of work zone at each end. One camera (Camera # 1) monitors the upstream traffic of the blocked lane and the downstream traffic of the un-blocked lane and collects vehicles arrival times (arriving at Line A), arriving-at-work-zone times (passing Line B), start-up lane shifting times (traveling between Line A and B), and queue discharge patterns for the blocked lane traffic and record the exit-work-zone-area times (passing Line B) for vehicles from the un-blocked lane; the other camera (Camera # 2) monitors exit-work-zone-area lane shifting times (traveling between Line C and D) and exit-work-zone-area times (passing Line C) for the blocked lane traffic, and arrival patterns and queue discharge patterns for vehicles from the unblocked lane. Travel time and speed data can then be estimated by fusing the two camera observations.

Simulation Data Collection

While field collected data is preferred, field observations may not be sufficient to support all desired analyses due to the high cost as well as the limits of observable work zone types and flow ranges. Therefore, simulation experiments from well-calibrated simulation models are needed. The research team proposes to use VISSIM to perform the simulation tasks.

Simulation experiments were conducted using the VISSIM microscopic traffic simulation package developed by PTV AG. This tool can be used to simulate and analyze traffic scenarios at a microscopic level with various traffic operation strategies and collect Measures of Effectiveness (MOEs) for transportation engineering and planning analyses. The flagger/temporal signal control methods can be simulated and controlled by the Signal State Generator (SSG). Also, VISSIM is capable of simulating discrete drivers' behaviors, e.g. alternative queue arrival and discharge patterns. Specifically, simulation experiments must be

designed to support the development of the work zone travel speed, queueing delay and capacity models.

Simulation Model Calibration

Simulation model calibration is critical for obtaining reliable simulation results and ensuring the simulated scenarios being compliance with realistic representations. In this study, field data collected from traffic sensors and video cameras is used to calibrate these models. Particularly, virtual loop sensors have been placed in the simulation model according to their real-world locations. Field observations at the traffic sensor locations were compared with virtual sensor measurements in the simulation environment for calibrating the simulation models. Calibration methods described in Zhang et al. (2009) will be applied in this study.

In VISSIM, each driver-vehicle unit is treated as an individual entity, and the traffic flow is modeled as a discrete and stochastic course which adjusts traffic parameters, e.g. headway time, vehicle arrival patterns, lane shifting time, start-up lost time, work zone travel speed, etc., according to the collected field data (ground truth). The simulation cycle is terminated or repeated depending on the comparisons between the simulation results and the corresponding field observations. The generated models are considered reasonably calibrated once the difference between the simulation results and the field observations is smaller than the pre-identified thresholds.

Once the simulation model is calibrated, it's ready for generating reliable data desired for various analyses. The following variables will be critical in producing simulation results for various scenarios to fill up the gaps of the field data. By assigning different values to these variables, various work zone configurations, traffic patterns, and control strategies can be simulated.

Work zone configurations

- Work zone length

- Posted speed limit

- Lateral clearance to work activities

Traffic flow characteristics

- Traffic flow type

- Arrival rate

- Vehicle type (truck percentage)

Signal/Flagger Strategies

- Fixed phases

- Demand driven phases (flagger control)

The efficiency of different traffic control methods can be evaluated by simply adjusting the signal/flagger strategies in the simulation model. Multiple simulation runs will be performed with different random seeds to minimize the deviation of simulation results and to ensure the simulation reliability. Both peak hour and off-peak hour traffic will be reflected by changing traffic demands. The commonly used MOEs such as throughput, work zone travel speed, average travel time, and roadway density will be collected as well. These MOEs will be combined with the field data for two-lane highway work zone capacity modeling and analysis.

3.2   Study Sites Selection

The selection of the study sites is based on the objectives of the two-lane highway work zone capacity analysis and the proposed data collection methods discussed earlier.

The work zone field data collection period is from May 2013 to November 2013, therefore, only the work zones under construction during this time period can be selected as potential sites. Table 2 provides the work zone property requirements for data collection. Considering the reality of work zone construction plans, certain types of work zone may not be available during the data collection period. In this case, simulation data will be used for the analysis.

The selected study sites are expected to have various work zone length, different control methods, over/under saturated traffic conditions, and percentage of heavy vehicles. For the lane closure work zone capacity analysis, the work zones with flagger and temporal signal control strategies is selected. For the non-lane closure work zone capacity analysis, the sites with advisory speed sign are preferred when such work zone data are needed.

TABLE 3-1 Property for two-lane highway work zone data collection

Work Zone Property	Requirements	Requirement Grade
Work zone duration	May, 2013 - November, 2013	Strictly required
Number of lanes	Two	Strictly required
Roadway type	Highway	Strictly required
Work zone location	On segments far from intersections	Suggested
Work zone length	Varies from 0.1 to 1 mile	Optional
Lane closure	Yes/No	Optional
Control method	Flagging/signal/pilot car/speed advisory sign/none	Optional
Traffic flow rates	Under/over-saturated	Optional

Note: 'strictly required' means the property is strictly required and no other alternatives can be accepted; 'suggested' means the property is required while the reality can be slightly different from the requirements; 'optional' means multiple alternatives need to be collected while fail-to-collect some of the options are acceptable.

The number of study sites with representative work zone and geometric configurations is determined subject to work zone duration and data collection possibilities. Only the work zones with good quality traffic detectors or possible video equipment set-up conditions are selected for field data collection.

The ideal number of study sites is six, while considering the realistic work zone construction plans in Washington State, approximately three to four lane closure work zones with different control methods and work zone length will be selected, and other alternatives will be simulated. Before-and-after (during) analysis is also expected to be conducted for non-lane closure work zone sites to estimate the work zone impacts on free-flow speed. Table 3 provides the ideal sites for lane closure work zones.

TABLE 3-2 Ideal site types for lane closure work zone capacity analysis

Site No.	Work Zone Length	Control Methods
1	Short	Fixed phases
2	Short	Maximum queue length
3	Short	Time gap out
4	Long	Fixed phases
5	Long	Maximum queue length
6	Long	Time gap out

According to Schonfeld and Chien (1999), the optimal work zone length for two-lane highway is 0.352 km (equals to 0.219 mi) when the traffic volume is 1,100 veh/h for the purpose of minimizing the total cost, including the agency cost and user delay cost. Therefore, the work zone length for modeling and analysis in this research is categorized into two categories, which are short (e.g., 0.1~0.5 mi) and long (e.g., 0.5~1 mi). Hence the significance of work zone length impact on driver behavior and work zone capacity can be tested; and the fixed phases control method, maximum queue length control method, time gap out control method can be tested and compared on the lane closure work zone sites.

3.3   Data Processing

In general, two types of data (field data and simulation data) are collected according to the data collection methods. The analysis will rely on field data wherever possible. Field data is

processed for quality assurance. The processed field data is used to calibrate the simulation models for reliable simulation experiments. For analysis scenarios without field observations, simulation data is employed.

For field data collection, traffic variables such as throughput, density, travel speed data, were collected from traffic sensors at the work zone areas. Individual behavioral data, such as vehicle arrival patterns, work zone travel time, and lane shifting time, were collected through video camera recordings properly configured at the study sites.

The simulation data was collected following the guidelines proposed in previous subsection. The simulation models will be calibrated based on the field data and all the work zone alternative scenarios will be simulated and the simulation data will be generated.

The field data obtained from traffic detectors and video cameras, and the simulation data generated by VISSIM were processed to extract variables needed by this study. Both the statistical data for the entire observation/simulation period and the 5- and 15-mininute statistical data for further model regression have been extracted. Example variables identified important for the two-lane highway work zone capacity analysis are as follows.

For the blocked lane

- Traffic flow volume and truck proportions

- Average/minimum/maximum lane shifting time on entry (for different flagger/signal control strategies)

- Average/minimum/maximum work zone travel time (for different speed limits)

- Average/minimum/maximum lane shifting time on exit (for different flagger/signal control strategies)

- Average/minimum/maximum queue length

- Average/minimum/maximum queue discharge time

- Average vehicle delay

- Direction capacity

For the un-blocked lane

- Traffic flow volume and truck proportions

- Average/minimum/maximum start-up lost time (for different flagger/signal control

strategies)

- Average/minimum/maximum work zone travel time (for different speed limits)

- Average/minimum/maximum queue length

- Average/minimum/maximum queue discharge time

- Average vehicle delay

- Direction capacity

3.4 Site Data Summary

Six sets of field data from different work zone sites were collected and processed for further

analysis and modeling. Table 3-3 summarizes the data collection schedule and basic work

zone characteristics.

TABLE 3-3 Actual data collection schedule for two-lane highway work zones

Work Zone No.	Route Name	Data Collection Date	Data Collection Period	Work zone Length	Intersections in between	Traffic Control
1	SR 278	JUN 07	7:00 AM – 9:00 AM	1572 ft	No	Flagger
2	SR 278	JUN 07	4:00 PM – 5:00 PM	2100 ft	No	Flagger
3	P-F Rd*	JUL 29	2:30 PM – 3:15 PM	800 ft	No	Flagger
4	P-F Rd*	JUL 29	3:15 PM – 5:00 PM	800 ft	No	Signal
5	P-F Rd*	AUG 14	12:30 PM – 1:30 PM	1000 ft	Yes	Flagger
6	P-F Rd*	AUG 19	2:15 PM – 3:15 PM	1~2 mi	No	Pilot Car

Note: P-F Rd refers to Preston-Fall City Road.

Traffic data in work zone #2 was incomplete due to a camera failure. Work zone datasets #3 and #4 were collected from the same work zone site. Signal control was used for work zone #4 so the recorded data type is different from other datasets. Work zone #6 was a moving project where work zone length was not fixed. Travel time data was not recorded for this site.

Datasets #1, #3 and #5 are mainly used in the data analysis and modeling. All datasets are used for model evaluation and simulation calibration.

Data Processing Result

Site photos for different work zones and data processing results are shown in the Appendix.

Arrival Pattern

Vehicle arrival patterns and headway distributions for all six work zone sites are shown in Appendix. The headway distribution graph shows that traffic flow is not uniform. Theoretically, at low traffic demands vehicle headway should follow an exponential distribution with λ equal to the traffic flow rate.

Lane Shifting Behavior

Field data also shows an impact of vehicle type on lane shifting time. Figure 3-3 shows an example of lane shifting time distribution for different vehicle types. The example is based on work zones #1, #3 and #5 as complete data is collected for those work zones. Observed data shows that the average lane shifting time is about 2.0 ~ 3.5 s. Heavy vehicles (truck & bus) are generally slower when starting up and shifting lane before work zone. But the difference

in lane shifting time is less significant in the after work zone shifting area as all types of

vehicles have already achieved the normal travel speed.
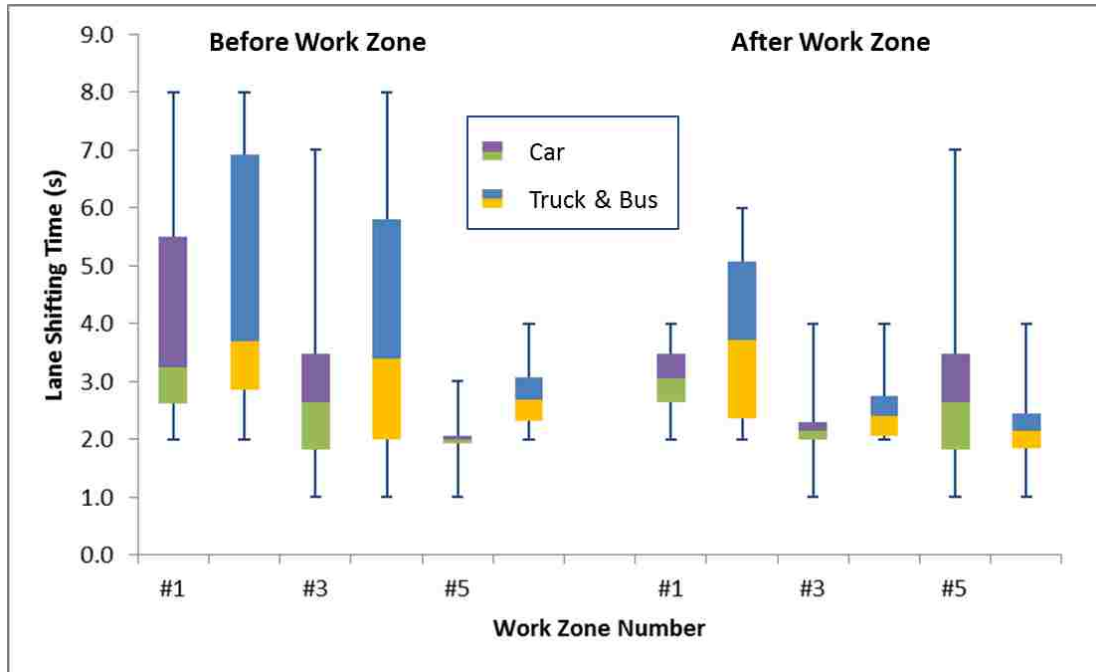
FIGURE 3-3 Impact of vehicle type on lane shifting time

Chapter 4   Capacity Model

4.1   Capacity Calculation

A mathematical model calculating two-lane highway lane-closure work zone capacity can be developed following the terminologies and equations from actuated signalized intersections.

In under-saturated conditions, the directional balance between vehicle arrival and departure can be expressed as:

$$q_i C = s_i g_{s,i} + q_i \left(g_i - g_{s,i} \right) \tag{4-1}$$

In the equation, directional traffic flow rate q_i (pc/h) is calculated by adjusting vehicle arrival rate (veh/h) in direction i ($i = 1$ or 2, representing two directions, respectively) with the directional heavy vehicle percentage. The left side of Equation (4-1) represents the total number of vehicles arriving at the work zone entrance for direction i, and the right side represents the total number of departure vehicles for the same direction. The second term in the right side represents the number of vehicles arrive after queue discharge and before the effective green time is ended.

When demand goes up to over-saturated levels, departure rate will be the saturation flow rate through the entire effective green time duration and Equation (4-1) can be re-written as

$$q_i C = s_i g_i \tag{4-2}$$

In over-saturated conditions, the directional flow rate q_i is lower than the arrival rate in direction i, causing un-cleared queues at the oversaturated direction.

As the focus of this study is the capacity of two-lane highway lane-closure work zone capacity, our interest is the scenarios when demand is close or even exceed the work zone capacity. Thus, without losing generality, Equation (4-2) will be used in this study. In over-

saturated conditions, work zone traffic control will be busy alternating the right of way for queue discharges or reduction.

The cycle length C in Equation (4-2) can be calculated using

$$C = r + g_1 + g_2 + L \qquad (4\text{-}3)$$

Signal cycle is composed of green signals, all-red time and total lost time. Effective green time (g_1 and g_2) is the portion of green and yellow when traffic movement could proceed at the saturation flow rate; all-red time is the time needed for vehicles travel though the open lane adjacent to the construction area; and total lost time includes the start-up lost time and clearance lost time for both directions.

Vehicles need a very long clearance time to travel through the lane adjacent to the construction area. The total all-red time per cycle is determined by the length of work zone and vehicle travel speed.

$$r = \frac{l}{V_1} + \frac{l}{V_2} \qquad (4\text{-}4)$$

From Equations (4-2), (4-3), and (4-4), the required directional effective green time can be calculated as

$$g_1 = \frac{s_2 q_1 \left(\dfrac{l}{V_1} + \dfrac{l}{V_2} + L \right)}{s_1 s_2 - s_2 q_1 - s_1 q_2} \qquad (4\text{-}5)$$

$$g_2 = \frac{s_1 q_2 \left(\dfrac{l}{V_1} + \dfrac{l}{V_2} + L \right)}{s_1 s_2 - s_1 q_2 - s_2 q_1} \qquad (4\text{-}6)$$

According to Equations (4-5) and (4-6), directional green time is mainly affected by vehicles arrival rates and saturation flow rates for both directions. The required effective green time is positively related with the traffic demand in the same direction and the saturation flow rate in the opposite direction.

Combining Equations (4-2) to (4-6), direction saturated traffic flow rate (which is also the directional capacity) at the work zone section can be calculated as

$$c_1 = \frac{s_1 g_1}{\dfrac{l}{V_1} + \dfrac{l}{V_2} + g_1 + g_2 + L} \tag{4-7}$$

$$c_2 = \frac{s_2 g_2}{\dfrac{l}{V_1} + \dfrac{l}{V_2} + g_1 + g_2 + L} \tag{4-8}$$

The total capacity of both directions is

$$c_{total} = c_1 + c_2 = \frac{s_1 g_1 + s_2 g_2}{\dfrac{l}{V_1} + \dfrac{l}{V_2} + g_1 + g_2 + L} \tag{4-9}$$

Equation (4-9) gives a mathematical estimation of the total capacity. For a certain work zone project where l, V, L, and s are fixed, the total capacity for the open lane is always lower than the saturation flow rate s. Total capacity increases with effective green time ratio in a cycle. Maximizing total capacity requires setting the portion of total green time, particularly g_i, as high as possible. If g_i is set as infinite, which means that the open lane only serves direction i, the total capacity approaches its maximum value, i.e. the saturation flow rate s. But in this case the right-of way is only allocated to one direction and vehicles in the other direction will suffer infinite delay. Therefore, the optimal traffic control plan needs to balance between the total capacity and vehicle delay.

A quantitative estimate of the capacity requires directional saturation flow rate, speed, and green time. However, these data may be difficult to collect in the field. In the following section, the mathematical models used to estimate these variables are presented. Analysts must note that, in capacity calculation, the field data is always preferred if the field observation is obtainable.

4.2   Estimating Model Parameters

Average Travel Speed

Directional work zone average travel speed is used in the equation calculating the cycle length. In HCM 2010, average travel speed (ATS) for two-lane highway is estimated using Equation (4-10) (combining Equation 15-2 and Equation 15-6 in HCM 2010).

$$V_i = BFFS - f_{LS} - f_A - f_{demand,i} - f_{np,ATS} \qquad (4\text{-}10)$$

where

$f_{demand,i} = 0.00776\left(v_{1,ATS} + v_{,ATS}\right)$, where $v_{1,ATS}$ and $v_{2,ATS}$ refer to the demand flow rate in pc/h/ln for the analysis direction and opposite direction, respectively (mi/h)

The demand adjustment factor $f_{demand,i}$ measures the influence of interactions of traffic demand for both directions on average travel speed. Impact of grade is also considered in this factor. For the two-lane highway work zone lane-closure scenario, opposing demand is 0 and there is no interaction between the analysis and opposite directions. So speed impact from the opposite traffic demand does not exist and $f_{demand,i}$ should be 0. Our analysis based on data collected in this study also suggests that directional demand flow rate has no effect on average travel speed. So f_{demand} can be taken out from the model for this specific two-lane highway lane-closure work zone speed analysis.

The no-passing zone adjustment factor $f_{np,ATS}$ is determined by opposing traffic demand and percentage of no-passing zones. For this research scenario, opposing demand is 0 and percentage of no-passing zones is 100% as only one lane is open for the work zone area. The adjustment for no-passing zone percentage is a constant speed reduction of 2.4 mi/h.

Base free-flow speed is essential in calculating average travel speed. HCM 2010 recommends that *BFFS* can be roughly estimated based on the posted speed limit. Although some other roadway characteristics such as curvature and grade may also affect the travel speed, it is difficult to quantify these factors for a long work zone site. The speed limit is used in the model to address the effect of these factors.

According to the observed data shown in Figure 4-1, the actual work zone travel speed is approximately half of the posted speed limit. Average travel speed for direction 1 is always a little lower than that for direction 2. There is a significant reduction in average travel speed compared to the speed limit.
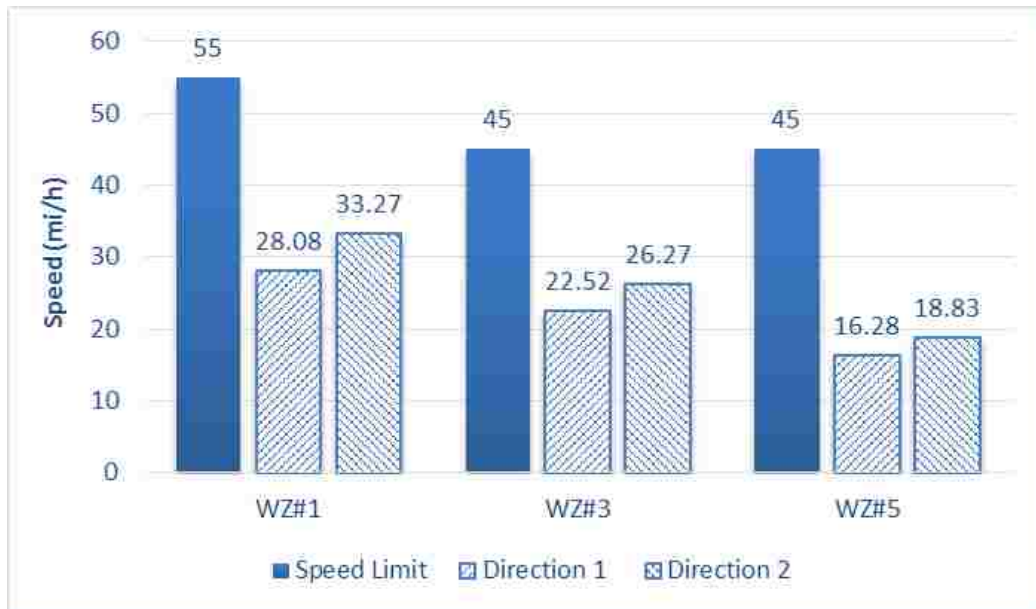
FIGURE 4-1 Work zone travel Speed for different sites

In the six work zones observed, most of the lanes are 12 ft in width. Shoulder width varies from 3.5 ft to 4 ft. Work Zone #5 has two access points located on the same side of the road. The distance in between is 350 ft. Here we doubled the access-point density number to find the adjustments as the HCM 2010 adjustments are based on the total density of two directions when both directions are open.

Tables 4-1 and 4-2 show the HCM adjustments reflecting the effect of lane width, shoulder width, and access-point density. These adjustments are used specifically for two-lane highway, which is different from studied work-zone scenarios. Values of the specific adjustments may also be slightly different. In the speed estimation we apply the HCM 2010 adjustments and use limited site data to verify the approach.

TABLE 4-1 Adjustments to FFS for lane and shoulder width

Lane Width	Shoulder Width (ft)			
(ft)	$\geq 0\ <2$	$\geq 2\ <4$	$\geq 4\ <6$	≥ 6
$\geq 9\ <10$	6.4	4.8	3.5	2.2
$\geq 10\ <11$	5.3	3.7	2.4	1.1
$\geq 11<12$	4.7	3.0	1.7	0.4
≥ 12	4.2	2.6	1.3	0.0

Source: HCM 2010. Exhibit 15-7

TABLE 4-2 Adjustments to FFS for access-point density

Access Points per Mile (Two Directions)	Reduction in FFS (mi/h)
0	0.0
10	2.5
20	5.0
30	7.5
40	10.0

Source: HCM 2010. Exhibit 15-8

The proposed average travel speed calculation takes the form as:

$$V_i = BFFS - f_{LS} - f_A - f_{np,ATS} \tag{4-11}$$

where $f_{np,ATS} = 2.4\ \text{mi}\,/\,\text{h}$ is a constant speed reduction.

And *BFFS* can be estimated based on the posted speed limit.

$$BFFS = \beta_0 + \beta_1 \times SL \tag{4-12}$$

where SL = speed limit of the two lane highway segment (mi/h).

Table 4-3 shows the regression result. The intercept β_0 is removed from the final model since it is not significant. Regression result after β_0 has been removed is shown in Table 4-4.

TABLE 4-3 Regression result for average travel speed model

	Estimate	Std. Error	t value	Pr(>|t|)
β_0	2.263	3.190	0.709	0.529
$\beta_{1,1}$	0.569	0.066	8.621	0.003
$\beta_{1,2}$	0.646	0.066	9.791	0.002

TABLE 4-4 Revised regression result for average travel speed model

	Estimate	Std. Error	t value	Pr(>|t|)
$\beta_{1,1}$	0.615	0.0084	72.91	0.000000212
$\beta_{1,2}$	0.692	0.0084	82.07	0.000000132

The final proposed average travel speed model is presented for consideration. The model estimates ATS based on the speed limit, lane and shoulder width, and access-point density.

$$V_1 = 0.615 \times SL - f_{LS} - f_A - f_{np,\,\mathcal{A}TS} \tag{4-13}$$

$$V_2 = 0.692 \times SL - f_{LS} - f_A - f_{np,\,\mathcal{A}TS} \tag{4-14}$$

The comparison between the model predictions and observed speed values is summarized in Table 4-5. The predicted ATS is quite close to the field observation.

TABLE 4-5 Comparison between model result and observed speed

No.	Direction	Observed ATS (mi/h)	Predicted ATS (mi/h)	Prediction Error
1	1	28.08	28.53	1.6%
	2	33.27	32.77	-1.5%
3	1	22.52	22.87	1.6%
	2	25.77	26.34	2.2%
5	1	16.28	15.37	-5.6%
	2	18.83	18.84	0.1%

Total Lost Time

Total lost time per cycle includes start-up lost time and clearance lost time for both direction. It can be expressed as

$$L = t_{s,1} + t_{c,1} + t_{s,2} + t_{c,2} \qquad (4\text{-}15)$$

where

$t_{s,i}$ = start-up lost time in the analysis direction (s)

$t_{c,i}$ = clearance lost time in the analysis direction (s)

The start-up lost time depends largely on first couple of car driver's reactions to the flagger's changing the right of way. However, since it only contributes to a small portion of the total work zone cycle length and the average start-up lost time are somewhat consistent, it is appropriate to treat start-up lost time as a constant and this simplification will not affect the result significantly. So, for a given work zone type, the start-up lost time is treated as a constant value in this study. The proposed model is capable of considering a different start-up lost time for each travel direction.

The clearance lost time represents the portion at the end of yellow signal that is not utilized. This is caused by drives' anticipation of the red signal.

In HCM 2010, the default start-up lost time recommended is 2.0 s, and the default value for clearance lost time is 2.0 s. Thus the default total lost time is 8.0 s. The capacity model takes thes value if field measurements are not available.

Saturation Flow Rate

Saturation flow rate refers to the queue discharge rate when the signal turns into green. The estimation of saturation flow rate *s* relies on the HCM 2010 and previous related research. Washburn et al (2008) proposed a saturation flow rate model for the two-lane highway lane-closure work zone scenarios:

$$s_i = \frac{3600}{\hat{h}_i}$$
$$\hat{h}_i = h_0 \cdot f_{speed} \qquad (4\text{-}16)$$

where

$\hat{h}_i = $ adjusted headway (s)

$h_0 = 3600/1900 = 1.89$ 燃 refers to the base headway calculated by the base saturation flow rate 1900 pc/h recommended by HCM 2010

$f_{speed} = 1 - 0.005\left(Min\left(V_i, ?5\right) - 45\right)$ is the average travel speed adjustment

4.3   Delay Estimation

As discussed before, the traffic control plan optimization needs to achieve a balance between roadway capacity and vehicle delay. Thus delay estimation is required for control analysis. Follow the HCM intersection control delay calculating equations, directional mean vehicle delay caused by two-lane highway work zone projects can be represented as

$$d_i = d_{1,i} + d_{2,i} + d_{3,i} \qquad (4\text{-}17)$$

Equation (4-17) is basically Equation 18-19 from HCM 2010. In this study, we assume no signal progression and no initial queue, which fits the situation of two-lane highway work zones. Thus $d_{3,i}$ could be taken out from the equation.

Deterministic delay term and random delay term can be calculated using the Equations (2-7) and (2-8) summarized in the literature review chapter. The directional mean vehicle delay is predicted by Equation (2-9), which is also presented in Equation (4-18). Mean vehicle delay for pre-timed signal control work zones can be calculated using a similar equation for signalized intersections when all signal timing variables are defined in the same way.

44

$$d_i = \frac{C\left(1 - \dfrac{g_{s,i}}{C}\right)}{2\left(1 - X_i \dfrac{C}{g_{s,i}}\right)} + 900T\left((X_i - 1) + \sqrt{(X_i - 1)^2 + \dfrac{mkI}{cT}X_i}\right) \tag{4-18}$$

Values for k can be calculated by Equation 18-41 in HCM 2010. For fixed time

control, $k = 0.5$. Since the purpose for calculating delay here is to identify the optimal

effective green time which is assumed repetitive for each cycle, $k = 0.5$ is recommended for

Equation (4-18). I incorporates the effects of metering arrivals from upstream signals. If the

control signal of the two-lane highway work zone is isolated, $I = 1.0$. The vehicle arrival

adjustment factor, m, accounts for the randomness in vehicles arrival. In the model validation,

it is tested with different values to address the specific vehicle arriving in two-lane highway

work zones.

The average delay for each vehicle is calculated as the summation of the directional

total delays divided by the total number of vehicles arrived. The calculated mean vehicle

delay is still in the unit of second per vehicle (s/veh).

$$d = \frac{(d_{1,1} + d_{2,1})Q_1 + (d_{1,2} + d_{2,2})Q_2}{Q_1 + Q_2} \tag{4-19}$$

As directional capacity increases with green signal length, the minimum required

green time, which represents the green signal length that can exactly serve the prevailing

traffic, can be calculated. The minimum required green time also corresponds to the

saturation status. To ensure that the vehicle queue can be fully discharged in each cycle,

saturated green time must not exceed the effective green time (4-20).

$$g_{s,i} \leq g_i \tag{4-20}$$

Substituting Equations (4-1) and (4-3) into (4-20), the directional effective green time

length must satisfy:

$$g_i \geq g_{i,\min} = \frac{q_i}{s_i - q_i}\left(C - g_i\right) \qquad\qquad (4\text{-}21)$$

Equation (4-21) gives the minimum required green time for the two directions. If directional green time is not long enough for queue dissipation, vehicles will accumulate before the signal heads. This makes delay increase over time.

One thing to note is that the minimum required green time may not a good control strategy. When minimum required green time is applied, directional capacity exactly equals to the demand. In practice as traffic flow is not deterministic, this is not a robust control solution. The control system balance is easy to break down. In later chapters, simulation experiments also indicate that the minimum delay is not achieved by minimum required green time. The optimal control plan should set the green time longer than the minimum green time.

Although the delay model can now be applied, it's still questionable whether it will provide accurate delay estimations for two-lane highway work zone scenarios. In the model validation section, work zone control adjustment is applied to the model and delay estimations are compared with simulation output.

Chapter 5   Microscopic Simulation

5.1   Control Plans

Three kinds of work zone control plans were observed in our study sites (four work zone projects controlled by flaggers, one controlled by fixed time signals, and one controlled by pilot cars. The work zone capacity model captures the influence of different control plans by including cycle length and green time in the equations. Pilot car control plan is not included in the simulation model as it does not follow a standard method and largely depends on specific work zone characteristics.

VISSIM traffic simulation models were built to evaluate impacts of different traffic control plans. While signal control plan can be directly implemented in the model, flagger control plan is not a standard module in the software. The research team successfully incorporated flagger control into the VISSIM traffic simulation model using the Vehicle Actuated Programming (VAP) interface.

In practice, flagger-based control plans are widely implemented by two-lane highway lane-closure work zone projects. Flagging operations can be described as follows: one operator (flagger) controls the signal using a flag or sign at each end of the work zone area for the bi-directional traffic flows. If a vehicle queue at one end is fully discharged, the operator at this end raises the red flag and switches the right of way to the other direction.

Signal-based control plans are similar to those of two phase controlled signalized intersections.

5.2   Model Input

Simulation model is based on work zone #3 and #4 due to little missing data and relatively

moderate traffic demand for these two sites. Flagger control and fixed-time signal control

were both observed, which provides adequate data to validate the model.

Roadway Characteristics

- Lane width: 12 ft

- Lane shifting area length: 168 ft/70ft

- Work zone length: 800 ft

Traffic Parameters

TABLE 5-1 Traffic parameters for simulation input

Direction	Traffic Demand (veh/h)	Truck Percentage	Speed Limit (mi/h)
1	261	5.0%	45
2	328	8.7%	45

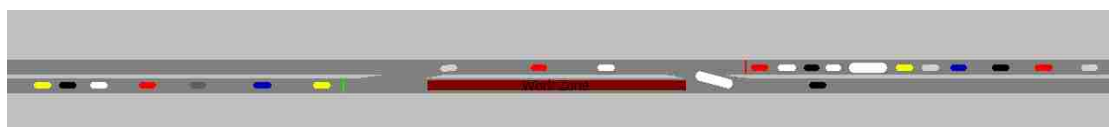The layout of the simulation model is shown in Figure 5-1.

FIGURE 5-1 Simulation model layout

5.3   Flagger Control Modeling

In VISSIM simulation modelling, the flagger control method can be modelled as an actuated

intersection, in which the gap time determines when to switch direction. A detailed

explanation for the logistic of this control plan can be described as follows:

- When all vehicles from the opposing direction have travelled through the work zone area, and no vehicles remain in the shared lane, the signal for this direction turns green and the vehicle queue starts discharging.

- When the vehicle queue has been fully discharged and there are no vehicles within the gap time interval of the intersection, the signal turns red and gives the right of way to the opposing direction.

In order to successfully execute the control plan in the VISSIM model, three loop detectors are set to detect the vehicle existence within the work zone area and the gap-out distance for the two directions, respectively. Figure 5-2 shows the layout of the detectors.

FIGURE 5-2 Layout of detectors for flagged control

The lengths of Detector 1 and Detector 2 are gap-out distances for the two directions, and Detector 3 is placed in the shared lane next to work zone area to avoid vehicle conflicts. As long as it detects a vehicle traveling in the shared lane, vehicles of the opposite direction are not allowed to enter the area. For the work zones we tested, a constant fixed work zone length is assumed and thusly, the length of Detector 3 is also fixed. Lengths of Detector 1 and Detector 2 can be calibrated to generate a result very close to the observation.

5.4 Model Calibration

According to field data collected and variables used in the capacity and delay model, driving behavior parameters and control plan performance were used to calibrate the simulation model

Driving Behavior

Vehicle travel speed and saturation flow rate are important variables in the capacity model. In the model calibration process, vehicle speed distribution and driving model parameters were adjusted. Work zone travel time and vehicle headway after signal heads (which is also the queue discharge rate) is compared between simulation output and field observation.

VISSIM allows users to manually adjust the vehicle desired speed distribution. Based on observed vehicle travel speed distribution, vehicle desired speed for two directions were adjusted as shown in figures 5-3 ~ 5-4. Note that the simulated speed distribution always has higher speed values than observed ones. This is because desired speed, rather than actual travel speed, is adjusted in the simulation model. During simulation runs vehicles usually travel at a lower speed than the desired speed.
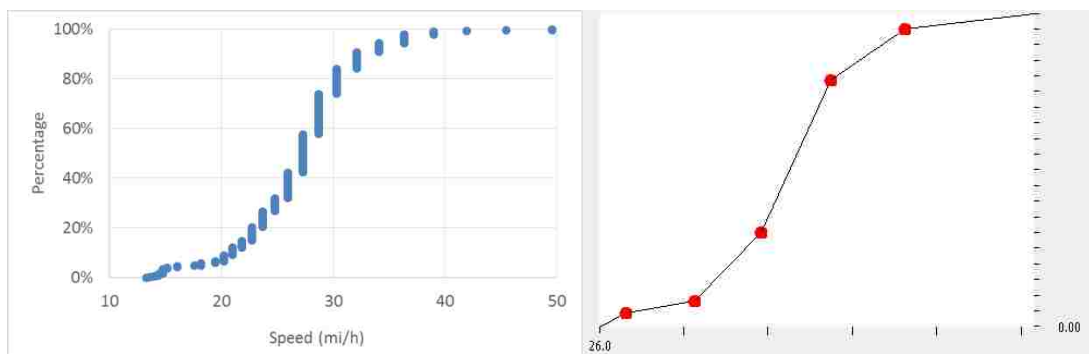
FIGURE 5-3 Observed vs. simulated speed distribution for direction 1
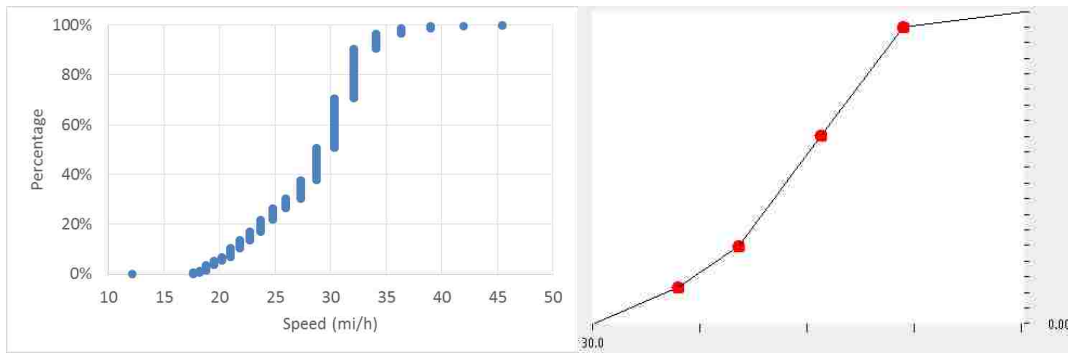
FIGURE 5-4 Observed vs. simulated speed distribution for direction 2

After adjusting driving model parameters and desired speed values, calibrated model result is shown in Table 5-2 and compared with observed data.

TABLE 5-2 Driving behavior calibration result

	Headway after Signal Heads		Work Zone Travel Time	
Direction	Simulation Result	Observed Value	Simulation Result	Observed Value
1	2.80 s	2.84 s	21.0	21.07
2	2.74 s	2.68 s	19.9	19.84

Figure 5-3 shows the impact of truck percentage on lane shifting time. Lane shifting time before work zone area increases with truck percentage. But for the lane shifting time after work zone area, the truck percentage does not have a significant influence. The model result is consistent with the field observation.
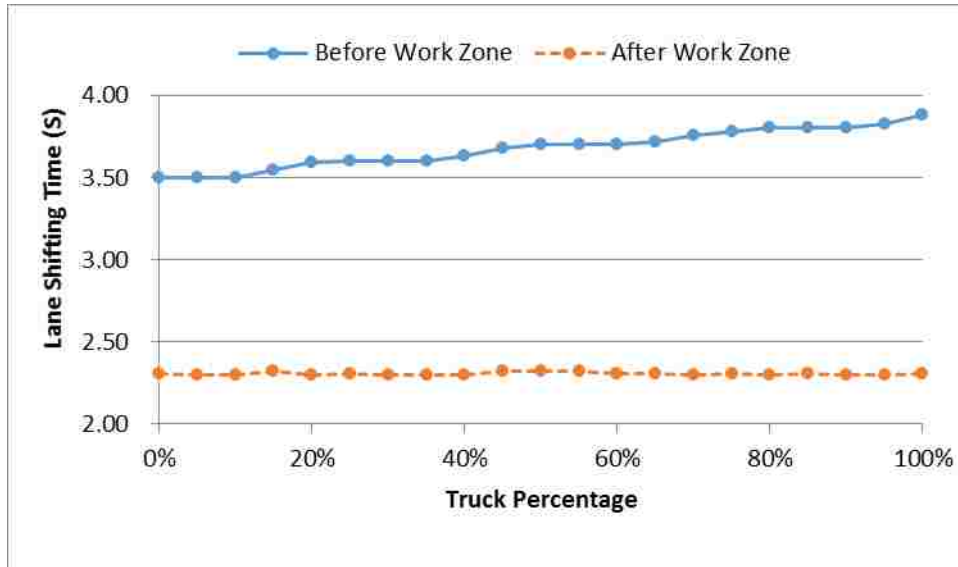
FIGURE 5-3 Simulated impact of truck percentage on lane shifting time

Control Plan Performance

Directional stop time and cycle length are compared in the calibration process and the optimal gap-out distance is defined as the value that generates the minimum average error. In the calibration we assume that two directions have the same gap-out distance, which means that the two flagging operators have the same vision.

Average stopped delay from field data and simulation model were compared to validate the accuracy of the calibrated VISSIM model. Percentage error (PE) was used to measure the difference between observed and simulated delay. If $\overline{D}$ stands for simulated delay, PE can be obtained following Equation (5-1).

$$PE = \frac{\left|\overline{D} - D\right|}{D} \times 100\%$$
(5-1)

Figure 5-4 shows the calibration results. The values of percentage error range from 0% to 33% for different gap-out distance. When the threshold value of gap-out distance is equal to 300 ft, the best goodness-of-fit is achieved with PE values of 4.1% and 0.4% for

direction 1 and 2 separately. In other words, the flaggers shifted right-of-way to opposite

direction when the distance between two approaching vehicles exceeding 300 ft.
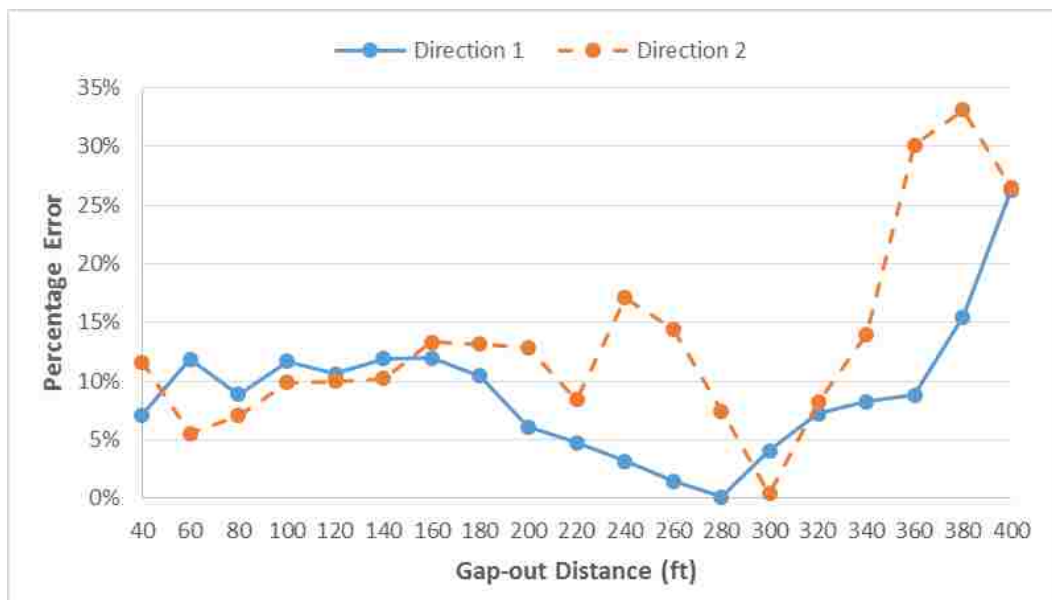
FIGURE 5-4 PE of stopped delay at different gap-out distance

The calibrated model result is shown in Table 5-3.

TABLE 5-3 Control plan calibration result

Direction	Gap-out Distance	Average Stop Time		Average Cycle Length	
		Simulation Result	Observed Value	Simulation Result	Observed Value
1	300 ft	38.2 s	38.6 s	128.6 s	127.5 s
2	300 ft	33.2 s	32.9 s		

Chapter 6　Delay Analysis

6.1　Mathematical Model Validation

Here we want to validate the mathematical model calculated vehicle delay with the calibrated simulation model. As proposed delay model is developed for signalized intersection delay estimation, it may not directly apply to two-lane highway work zones. To test the model accuracy, mathematical model predictions are compared with simulation results.

Twenty-four scenarios, with different traffic demands and control signal settings, have been tested for mathematical model validation. Each scenarios was simulated under 10 different simulation seconds. Each signal simulation time lasted for 7200 simulation seconds. A "warm-up" time is allowed in the simulation before averaging vehicle delays. For certain traffic demands, not all signal settings are applicable. If the green signal length is two short, it's unable to serve the prevailing traffic. In the simulation model vehicle queue may max-out of the links, thus the simulated delay results are not accurate. For each traffic flow condition, we tested the signal timing that have capacity greater or slightly smaller than the vehicle input. These corresponds to under-saturated or slightly over-saturated conditions. Traffic characteristics and work zone configurations are based on field observations at work zone #3. Scenarios with same traffic demands are shown in the same figure together. First we tested the delay prediction accuracy using $m = 8$, which is recommended in HCM 2010. Moderate traffic condition ($Q_1 = Q_2 = 300$ veh/h) is tested first as it's close to the real traffic demands.

FIGURE 6-1 Comparing model calculated delay and simulated delay

As shown in the figure, model calculated delay has a similar pattern as simulated delay. Minimum vehicle delay was achieved when green signal length is around 40 ~ 50 s for each direction. The mean absolute prediction error is 17.9%. Model calculated delay is always larger than the simulation result, which suggests a system error may exist. The differences decrease with the green signal length. Further look at the uniform delay and incremental delay diagram in Figure 6-2. Uniform delay is linear while incremental delay decreases with green signal length. Compare it with Figure 6-1, properly reducing the incremental delay may bring the mathematical calculated delay more close to the simulated values. This indicates traffic flow randomness has less impact on mean vehicle delay for two-lane highway work zones than signalized intersections. Thus smaller values for vehicle arrival factor, *m*, were tested.
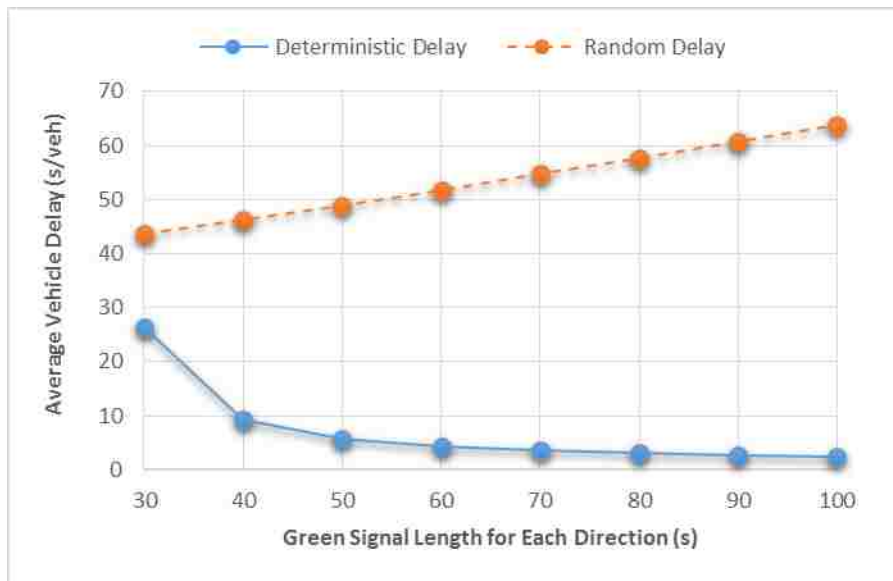
FIGURE 6-2 Deterministic delay and random delay

After testing different values, an accurate result can be achieved when $m = 2$. The delay result is shown in Figure 6-3. After applying the adjustment, the two curves become closer, with a mean absolute error of 1.6%. Mathematical model generated reasonably accurate predictions.
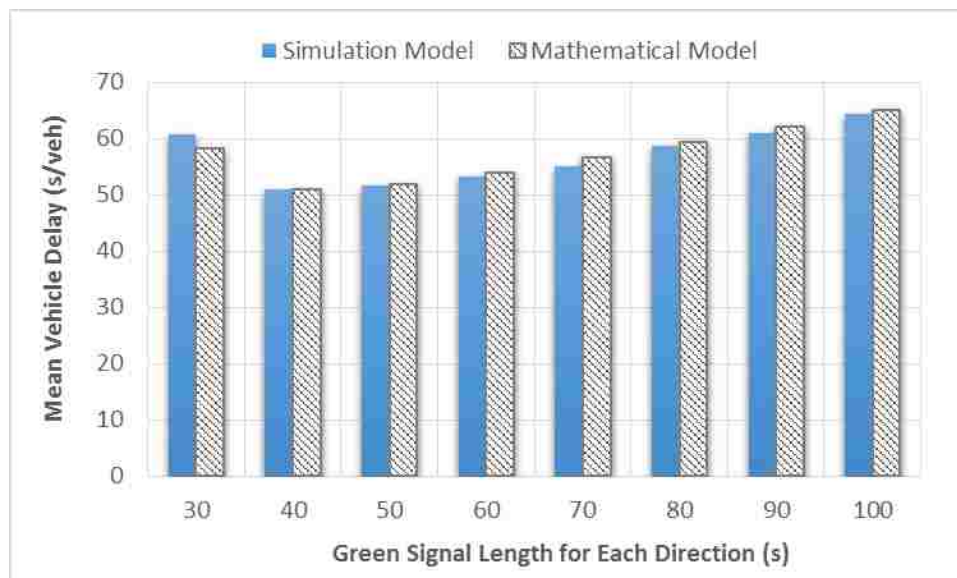
* Traffic Input: 300 veh/h, 5% trucks for each direction
* Optimal $m = 2$ with mean prediction error of 1.6%

FIGURE 6-3 Comparing adjusted model calculated delay and simulated delay

Delay comparison for two more traffic conditions were tested and presented in Figures 6-4 and 6-5. Vehicle delay under low traffic demands ($Q_1 = Q_2 = 200$ veh/h) and high traffic demands ($Q_1 = Q_2 = 400$ veh/h) were calculated and compared with simulation results. Study shows that $m = 2$ also gives the most accurate estimation for low traffic demands (with the mean absolute error of 1.6%). The most accurate estimation for high traffic demands happens when $m = 4$ (with the mean absolute error of 2.3%). Results are shown in Figures 6-4 and 6-5.

* Traffic Input: 200 veh/h, 5% trucks for each direction
* Optimal $m = 2$ with mean prediction error of 1.6%

FIGURE 6-4 Delay comparison under low traffic demands
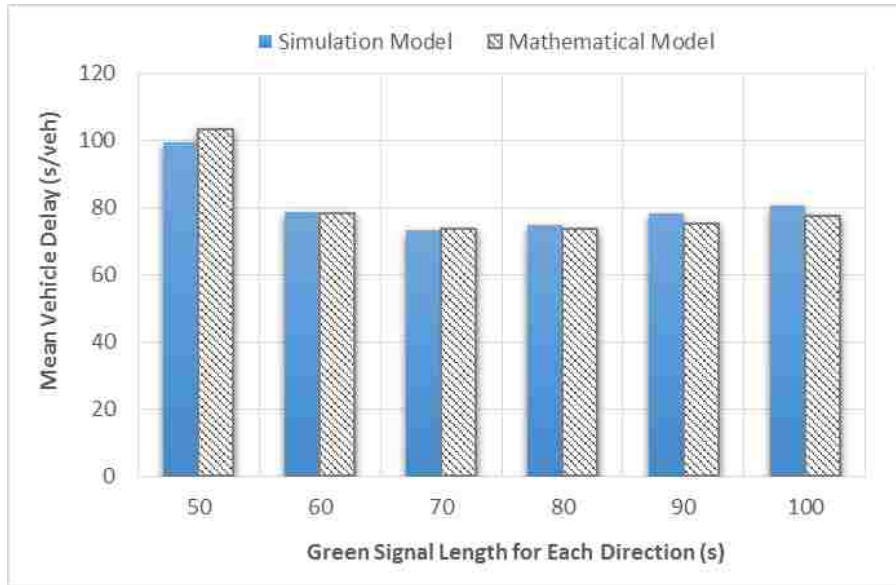
* Traffic Input: 400 veh/h, 5% trucks for each direction
* Optimal $m = 4$ with mean prediction error of 2.3%
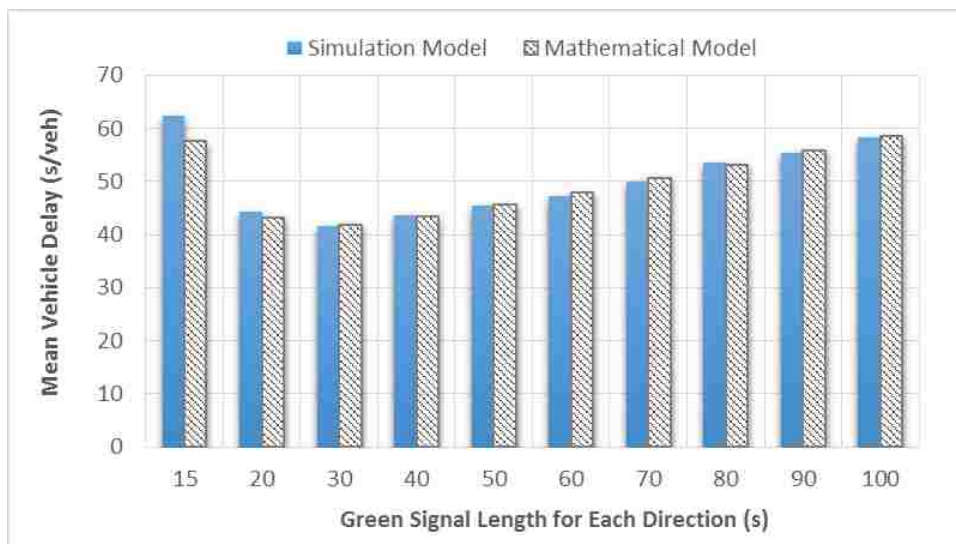
FIGURE 6-5 Delay comparison under high traffic demands

After adjusting the random arrival parameter *m*, the mathematical delay model can produce reasonable estimations, with mean prediction errors of 1% ~ 3%. The optimal values of *m* vary from 2 to 4, which is smaller than the HCM recommended value ($m = 8$). The study shows that the optimal *m* could be a function of traffic demand. For the traffic demand of 400 veh/h in each direction, the optimal *m* value is greater than lower traffic demands (200 veh/h and 300 veh/h in each direction). This indicates that randomness in higher traffic demand may cause greater stochastic delay.

6.2   Field Data Study

After model calibration, mathematical model and simulation model can be use together to study actual work zone sites. In this section, field observed traffic demands are used. Average traffic demands are used in calculation. Vehicle delays are estimated for different green signal lengths. Figure 6-6 shows the delay results. Each delay curve can be divided into two

segments. When the green time is too short to discharge the queue, users will experience very long delay time. In this segment, vehicle queue will accumulate over time. The minimum required green time, $g_{i,min}$, marks the turning point of the curve. In order to control the delay at a more stable level, green signal length should be longer than $g_{i,min}$, and vehicle queue for each cycle will be fully discharged. For fixed time signal control, the mathematical model provides a precise estimation for the microscopic simulation results.
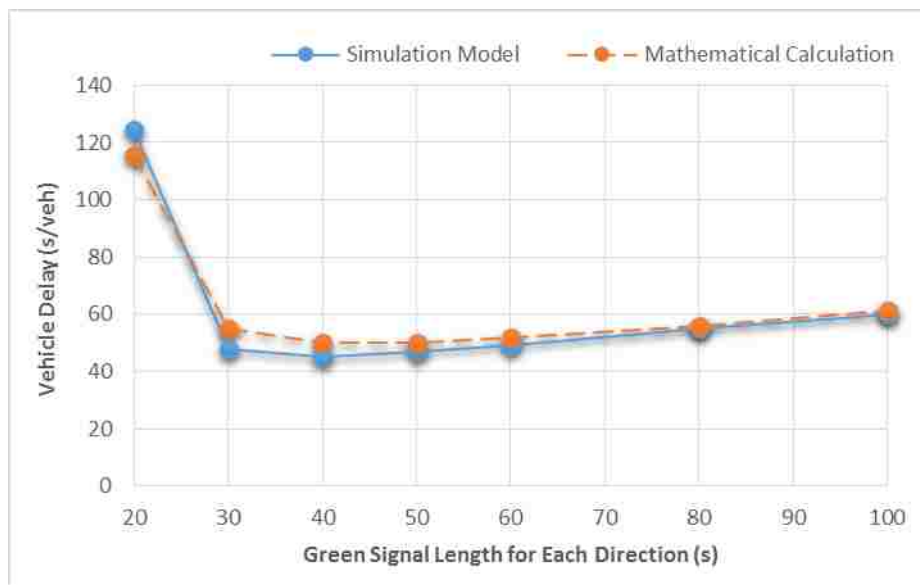
FIGURE 6-6 Delay comparison for field observed traffic demands

A comparison between pre-timed signal control and flagger control is also presented in Figure 6-7. Vehicle delays are estimated using the simulation model. Flagger control almost has the same $g_{i,min}$ as the fixed time signal control, and vehicle delay does not increase with a longer max-out green time. Using gap-out distance method, flagger control plan is more effective to control the vehicle delay at a very low level, which is nearly as good as the optimal result. Empirically observed green signal lengths for this site are usually around 40 ~ 50 s, when vehicle delay for flagger control is about 10% ~ 20% lower than pre-timed signal control.
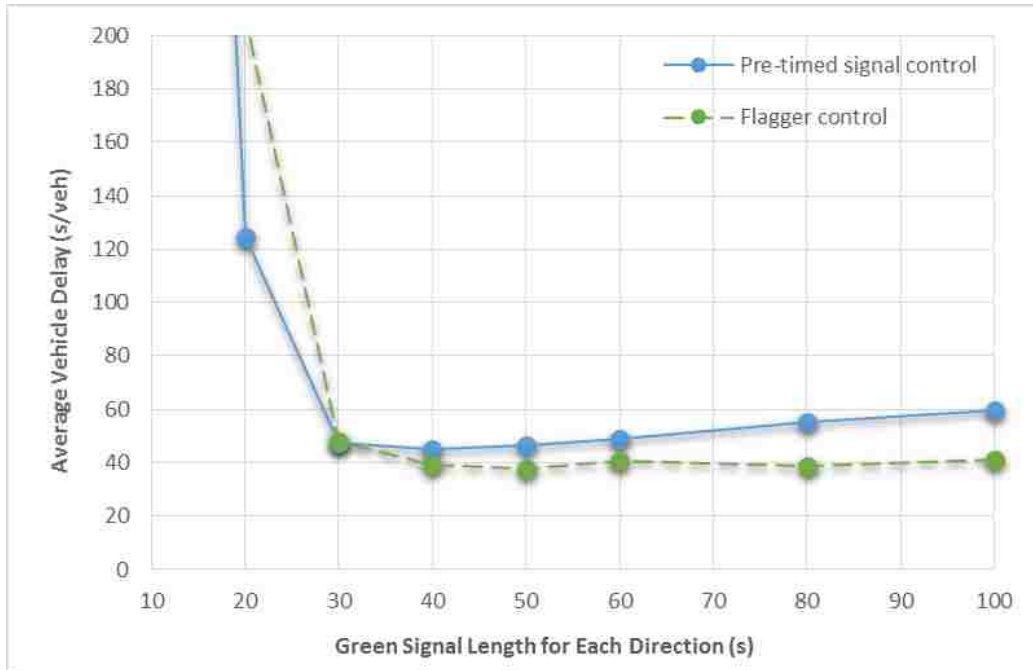
FIGURE 6-7 Comparison between pre-timed signal control and flagger control.

6.3   Effectiveness of Flagger Control

The calibrated simulation model can also be used to estimate delay for more traffic

conditions. Thirty-six scenarios are tested to analyze vehicle delay caused by flagger control.

Each scenarios was simulated under 10 different simulation seconds. Each signal simulation

time lasted for 7200 simulation seconds.

Figure 6-8 shows the flagger control delay diagram under multiple traffic demands

(200 ~ 600 veh/h). Five-percent of heavy vehicle percentage is assumed for both directions.

The flow rate values in the legend are the tested traffic demands for both directions.
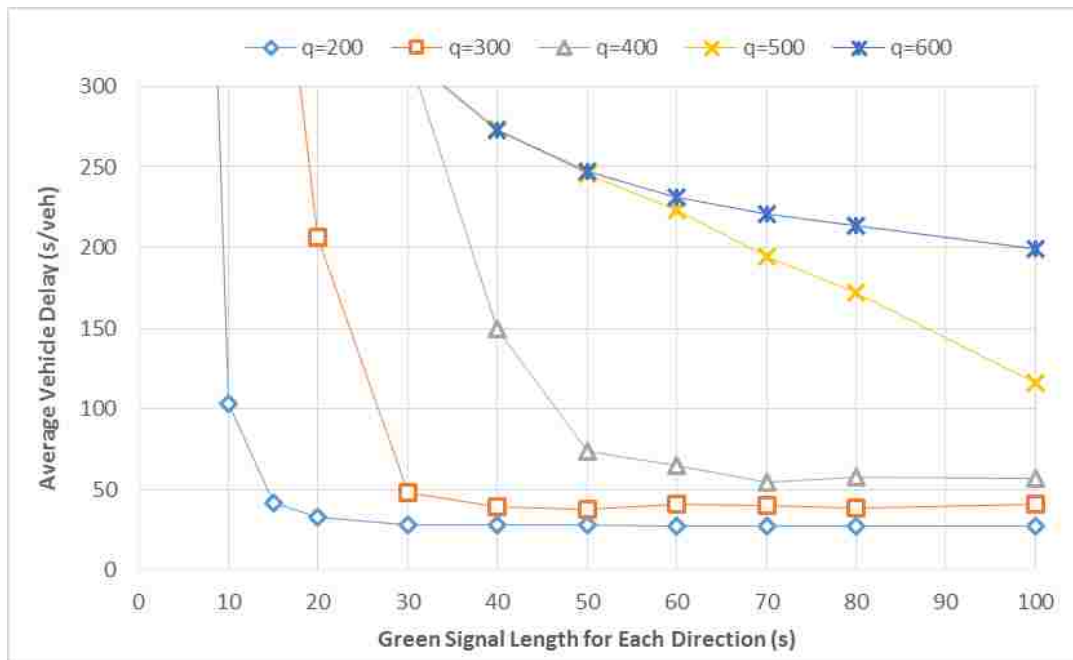
FIGURE 6-8 Delay diagram for multiple traffic demand levels under flagger control

From Figure 6-8, the minimum required green time increases with traffic demand. At low or normal traffic demands (200 ~ 400 veh/h), vehicle delay drops sharply before the minimum required green time. When the green signal length exceeds the minimum required green time, delay values keep at a stable level. This indicates that flagger signal length is cut in time when vehicle queue has been discharged, determined by gap-out method. At high traffic demands (500 ~ 600 veh/h), we cannot find a green signal length between 0 ~ 100 s capable to serve the traffic. It seems that the delay curves for flagger control has a sudden change when traffic demand increases to 500 veh/h. Flagger control is proven to be a stable traffic control plan when traffic demand is lower than 400 veh/h, but it does not perform well when traffic demand is higher.

6.4   Optimal Control Strategy

Based on previous discussions, an optimal control strategy for two-lane highway work zones can be proposed. When work zone configurations are decided, an optimal green signal length can been found from the delay diagram. For pre-timed signal control strategy, the optimal green signal length corresponds to the minimum average vehicle delay. Although it's extremely complex to take derivative of the delay model, traffic operators can try different green signal lengths and choose the value that gives the smallest average vehicle delay. As the mathematical delay model is validated, there is no need to build and calibrate the simulation model. However, the accuracy of the delay predictions still relies on estimations of saturation flow rate, work zone travel speed and start-up lost time.

For low traffic demands, flagger control is a stable solution considering minimizing user delay. If field data is not enough for delay calculation or signal facilities are difficult to set, operators can always seek help for flagger control to ensure low vehicle delay. As flagger control could also be considered as a kind of demand-driven control strategy, a similar actuated control algorithm could be designed to reach similar effects to avoid the high human cost. In our research, distance gap-out method is used to analogue the flagger strategy. In practice, time gap-out method is also effective as it works in a similar way as distance gap-out.

Chapter 7　Capacity Analysis

7.1　Capacity Calculation

Based on field observations, we can apply the capacity model and calculate the capacity for real work zone sites. Below is a calculation example for work zone #4, for which pre-timed signal control is used.

Observed data is summarized in Table 7-1. Saturation flow rate data is processed and calculated from video recordings.

TABLE 7-1　Field observations for work zone #4

Direction	Work zone Length (ft)	Average Travel Speed (mi/h)	Saturation Flow Rate (pc/h)	Green Signal Length (s)	Yellow Signal Length (s)
1	800	22.68	1292.3	40	8
2	800	26.14	1446.6	40	8

Calculation procedure is shown in Table 7-2. Note that speed has been transferred to the unit of ft/s.

TABLE 7-2　Calculation procedures for work zone #4 capacity

Direction	Average Travel Speed (ft/s)	Effective Green Time (s)	Direction Capacity (pc/h)	Total Capacity (pc/h)
1	33.26	44	415.3	880.1
2	38.34	44	464.9	

Based on our calculation, when effective green time is 44 s for both directions, the directional capacities for work zone #4 are 415.3 pc/h and 464.9 pc/h, respectively. The total capacity is 880.1 pc/h.

7.2　Sensitivity Analysis

A sensitivity test is conducted to analyze different variables' impact on the lane closure traffic control capacity. In the capacity model, directional capacity is determined by saturation flow rate, vehicle speed, work zone length and signal timing. In practice, saturation flow rate is usually determined by drivers' reaction time which is not very sensitive to work zone settings. Construction projects would greatly influence traffic through their lane closure area length, the impact of vehicle speed, and the implementation of traffic signals. In this section impacts of these three variables are analyzed based on the developed capacity model. Initial input values are from field observation. In the sensitivity test, different values of work zone length, average travel speed, and green time is tested independently.

Figure 7-1 illustrates how capacity changes with different work zone lengths. The total capacity monotonically decreases with work zone length. Directional capacities follow a similar pattern. Direction 1 always has a slightly lower capacity than direction two because of lower saturation flow rate and vehicle speed in direction 1. For short work zones, the slope of the capacity curve is greater, thus it's effective to gain capacity by reducing work zone length. But for long work zones, reducing work zone length would not bring as significant increase in capacity.
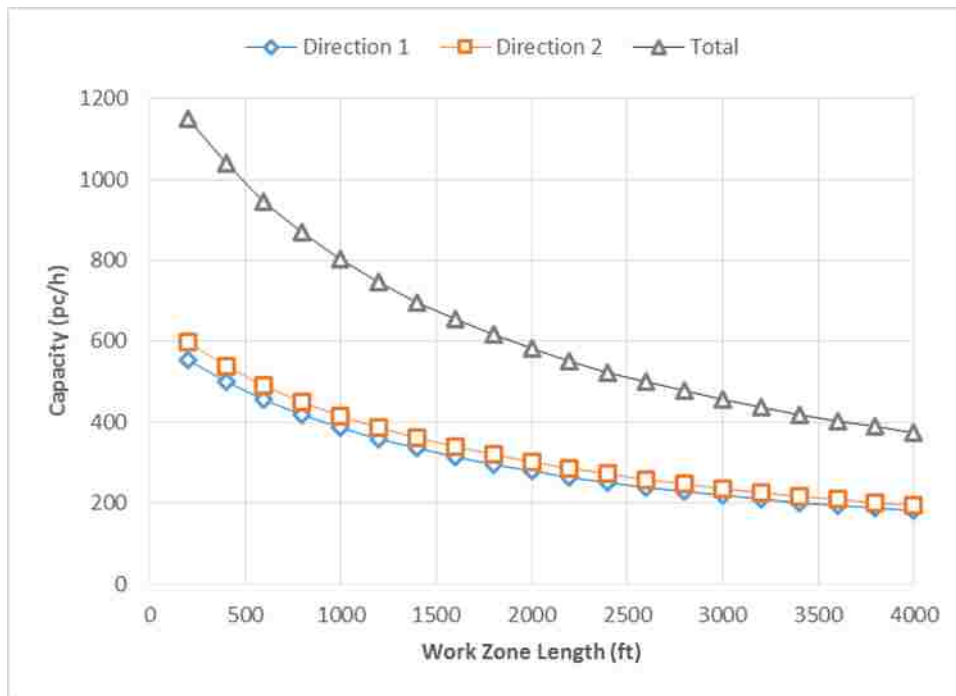
FIGURE 7-1 Impact of work zone length on total capacity

The impact of average travel speed on capacity is shown in Figure 7-2. Direction 1 speed is tested for different values while direction 2 speed kept unchanged. The graph shows direction speed does not have a specific influence on the directional capacity, as direction 2 capacity is always slightly higher than direction 1. The increase in direction speed only influences the clearance time (all red time) between green signals, so it has the same impact for two directions. Here we keep the saturation flow rate unchanged. In practice the saturation flow rate may also increase with the direction travel speed, which will have some positive effect on the directional capacity.
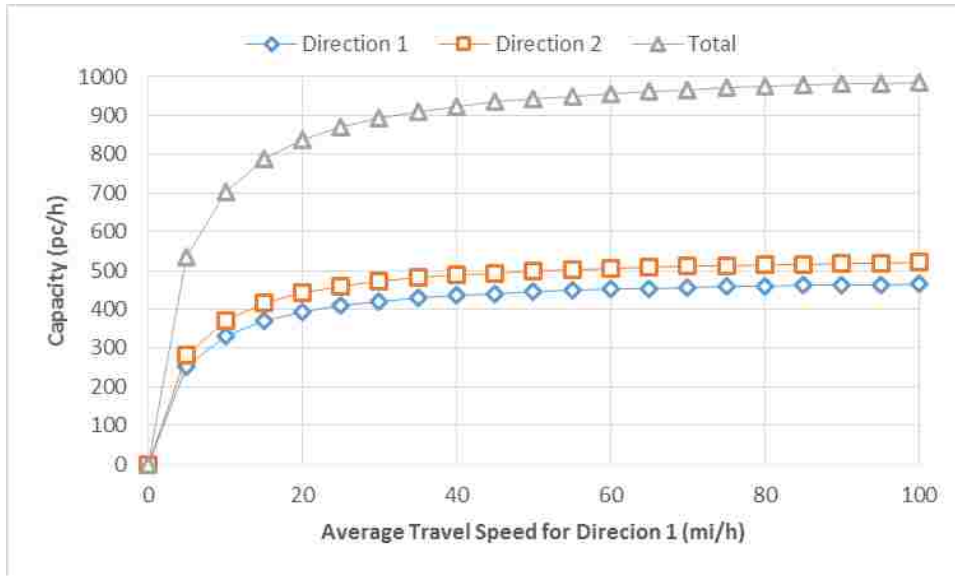
FIGURE 7-2 Impact of average travel speed on direction and total capacity

Although direction and total capacity increases with the speed, it's not the efficient way to gain capacity by increasing average travel speed. From the figure, when the speed is larger than 40 mi/h, there is little room for capacity increase. The main concern may be that traffic operators should make sure that vehicles' not travel though work zone travel at a very low speed by having enough lane width, lateral clearance and other related conditions.

Figure 7-3 shows the contour graph of changing average speed in both directions. The surface is almost symmetric by direction (not perfectly symmetric because the differences in directional speed and saturation flow rate). The surface shape indicates that total capacity is actually determined by the lower average travel speed in the two directions. As long as vehicles in one direction travel slowly, the total capacity will be at a very low level.
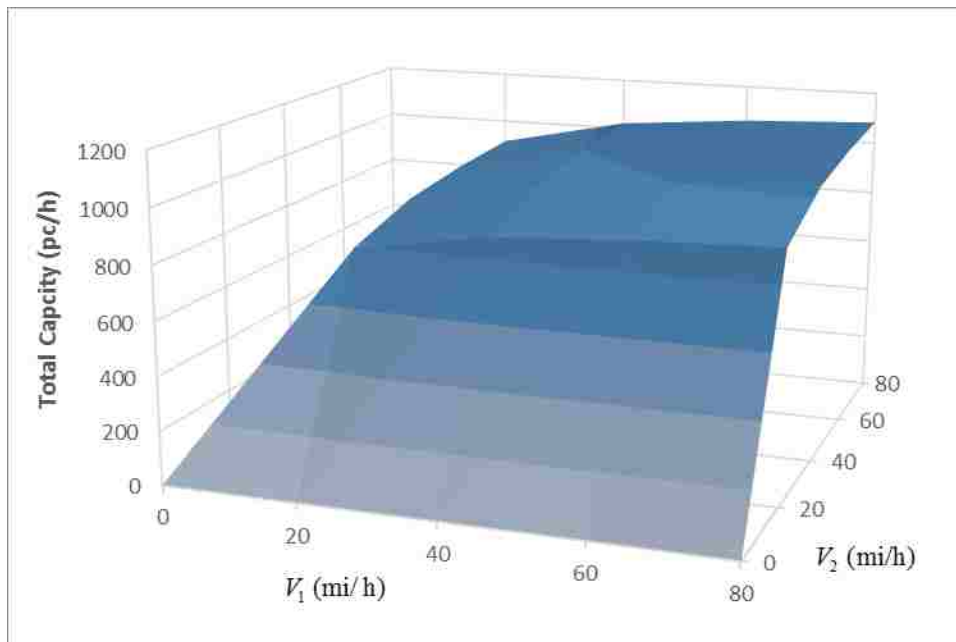
FIGURE 7-3 Contour graph of speed impact on total capacity

The impact of green signal length on capacity is shown in Figure 7-4. Direction 1 green time is tested for different values while direction 2 green time kept unchanged. By increase its green signal length, direction 1 capacity increases significantly with a drop in direction 2 capacity. Total capacity also increases as total green ratio in each cycle goes up. The balanced condition (two directions have the same capacity) does not corresponds to the highest total capacity value. Compared to the balanced condition, if the signal split is slightly unbalanced allocated based on the actual traffic demands, a larger total capacity can be achieved. A highly unbalanced signal allocation is not recommended considering the equity for drives in both directions.
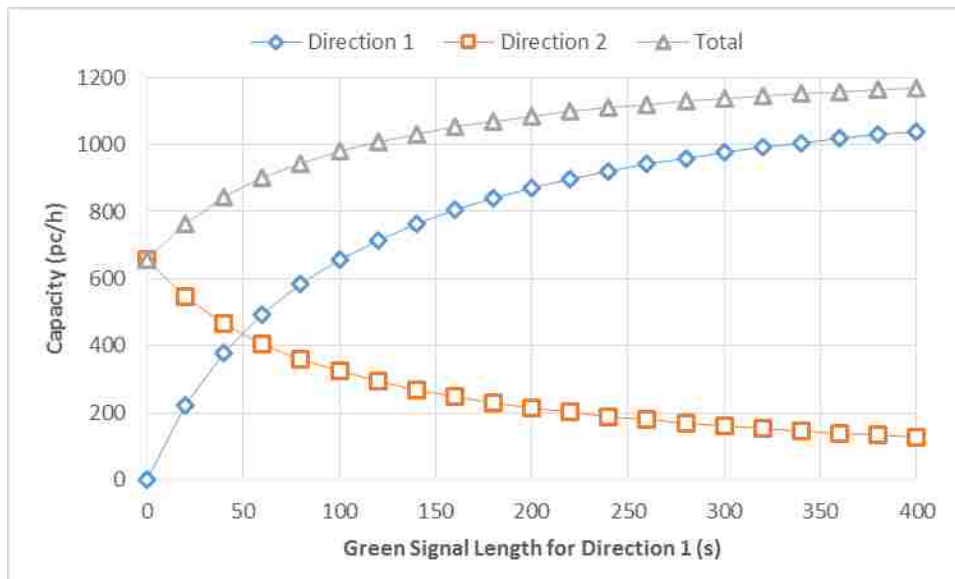
FIGURE 7-4 Impact of green signal length on direction and total capacity

Figure 7-5 shows the contour map of changing green signal lengths in both directions. The surface is also nearly symmetric by direction. The total capacity depends on the total green time in two directions. Increase the green signal length in any direction will always achieve some total capacity increase, but this capacity gain is direction specific. For example, increasing direction 1 green time will only result in an increase in direction 1 capacity, and also cause a small decrease in direction 2 capacity from previous discussion.
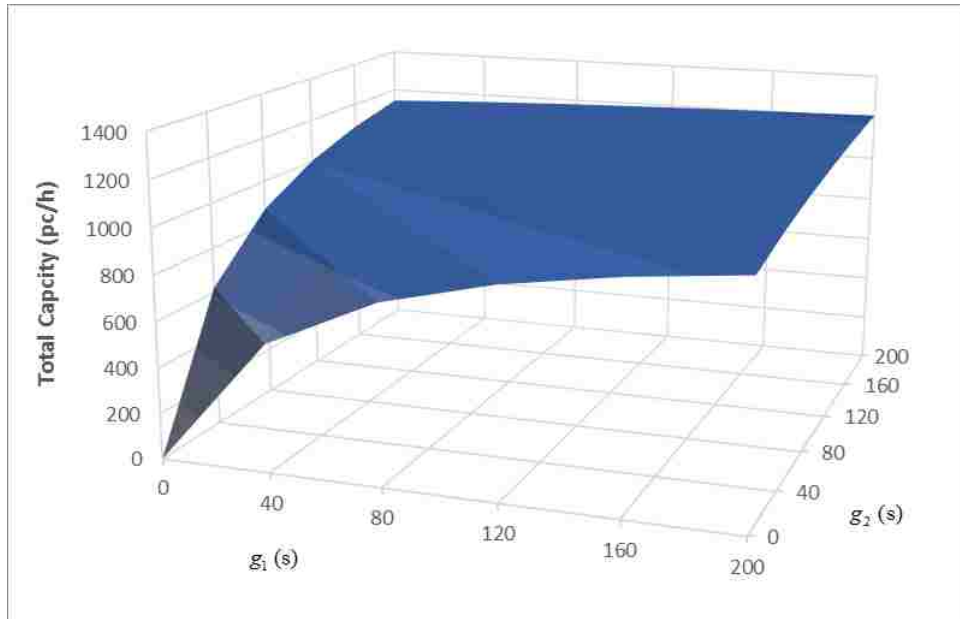
FIGURE 7-5 Contour graph of green time impact on total capacity

7.3   Relationship between Capacity and Delay

From the data above, we can observe delay varies with different green signal length. In the capacity model, signal program also determines the roadway capacity for a typical work zone site. Hence there exists some relationship between delay and capacity. More traffic scenarios are tested using the adjusted mathematical delay model. The mean vehicle delay to total capacity diagram is shown in Figure 7-6. Five percent of heavy vehicles is assigned for both directions. The capacity value in the horizontal axis is shown in the unit of passenger car per hour (pc/h). Applying the heavy vehicle equivalent factor of 1.5 for terrain grade two-lane highways, one vehicle is equivalent to 1.025 passenger cars.

69
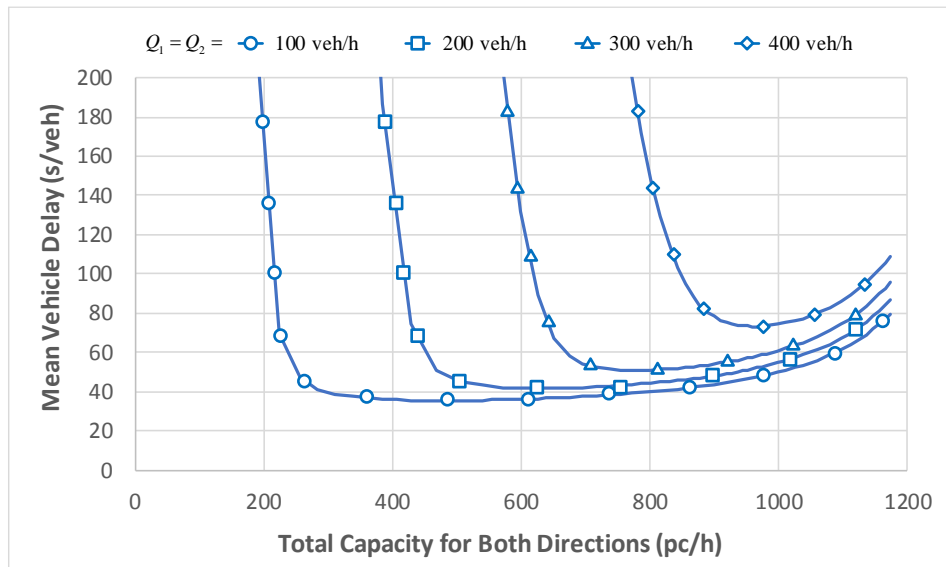
FIGURE 7-6 Relationship between total capacity and mean vehicle delay

Each delay curve shows that for a typical traffic flow condition, how mean vehicle delay changes with the capacity. In the analysis, different roadway capacity is only achieved by altering signal settings, which means that traffic characteristics such as saturation flow rate and travel speed keep unchanged. For each traffic condition, signal programs should be set to have a total capacity larger than the total traffic flow, in order to control delay at a relatively low level. In each curve, we can observe that mean vehicle delay is minimized somewhere in the middle. So for a certain traffic condition, there exist an optimal signal program that minimizes the average delay incurred by users. For low traffic demand (e.g. 100 veh/h in each direction), the optimal signal program is relatively easy to achieve. Any signal setting which gives a capacity around 400 ~ 600 pc/h would have similar effect as the optimal solution in terms of minimizing delay. For low traffic demand (e.g. 400 veh/h in each direction), the optimal signal setting corresponds to the total capacity around 950 pc/h, and if the capacity is set higher or lower, vehicle delay will increase significantly.

Chapter 8   Case Study: Unbalanced Traffic Flow

8.1   Unbalanced Traffic flow

Previous analysis is based on balanced traffic flow rates. In practice, it's unlikely to have exact equal traffic demands for both directions. Thus it is necessary to further examine unbalanced traffic flow scenarios. Several features related to unbalanced traffic flows are:

- Directional traffic flows may not have a very significant difference. From our field observations, the demand ratio is between 1:1 and 1:3.

- If just consider average delay time among all vehicles, it doesn't matter which direction has larger traffic demand.

- According to the green time calculation function, directional green time should have the same ratio as traffic demands.

An analysis example for unbalanced traffic flows is summarized in Figure 8-1. Simulation model is used to analyze flagger control delays for unbalanced traffic flows. The tested traffic flows are $Q_1 = 300 \text{ veh/h}$ and $Q_2 = 600 \text{ veh/h}$, which have a demand ratio of 1:2. Both directions have 5% heavy vehicles. Figure 8-1 shows the impact of maximum green time on vehicle delay. The maximum green time for direction 2 is always set as two times that of direction 1.
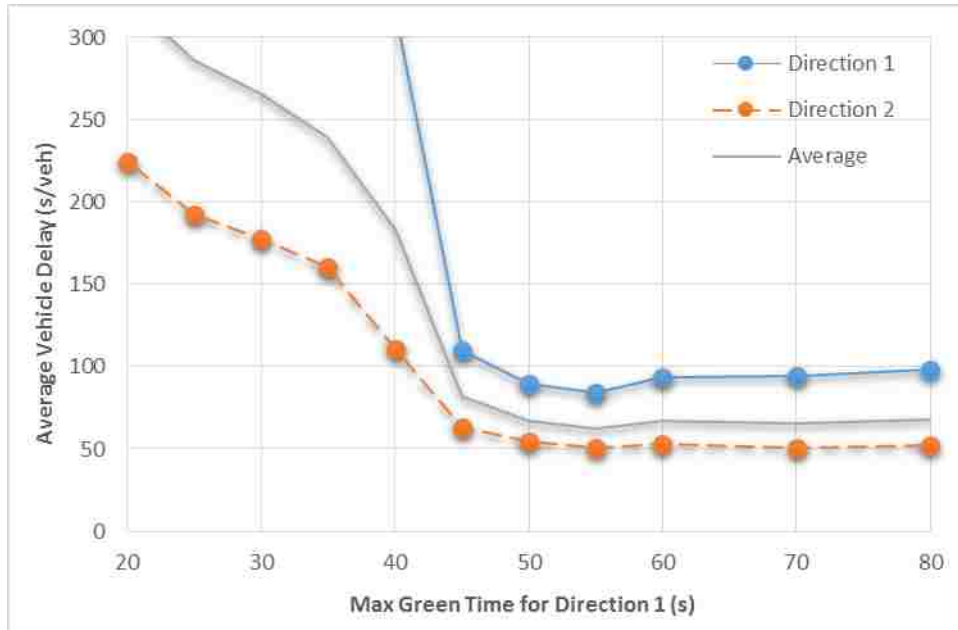
FIGURE 8-1 Delay diagram for unbalanced traffic flows

Compared with balanced conditions, unbalanced traffic flows also generate a similar delay curve. The optimal control plan that minimizes vehicle delay is 55 s of maximum green time for direction 1 and 110 s of maximum green time for direction 2. Vehicles in the direction with lower traffic demand have larger delay as opposite direction has longer green time.

In another example, two unbalanced traffic conditions, moderate traffic and heavy traffic, are analyzed. In each analysis example, the combined traffic rate and total max-out green time are fixed. The only variable is the traffic flow ratio, which is also the max-out green time ratio. The combined traffic rates are 600 veh/h and 800 veh/h, while the total green time lengths are 80 s and 120 s, respectively for the two examples. Traffic demand and green time is divided by ratios of 1:1, 1:2 and 1:3 between the two directions. Thus, directional traffic demands take values from 150 veh/h to 600 veh/h, which reflect most of the observed highway traffic rates. A directional traffic flow higher than 600 veh/h is not preferred, as it may exceed the directional capacity.

Figures 8-2 and 8-3 summarize the delay results. When traffic demands are unbalanced, vehicle delays are also unbalanced in two directions. Direction 1 is the direction always with a lower traffic flow rate. When the demand ratio changes from 1:1 to 1:3, vehicle delay for direction 1 becomes higher. Vehicle delay for direction 2, which has a higher traffic demand, decreases when traffic flows become more unbalanced. An interesting finding is that overall average vehicle delay is lower for unbalanced traffic, compared to balanced traffic demand. This is because unbalanced allocation of traffic and right of way is actually more efficient. An extreme case is that all traffic is in the same direction, then vehicles may keep travelling without stops. Comparing the moderate traffic with heavy traffic, two scenarios show similar conclusions, but the vehicle delay for heavy traffic is generally higher.
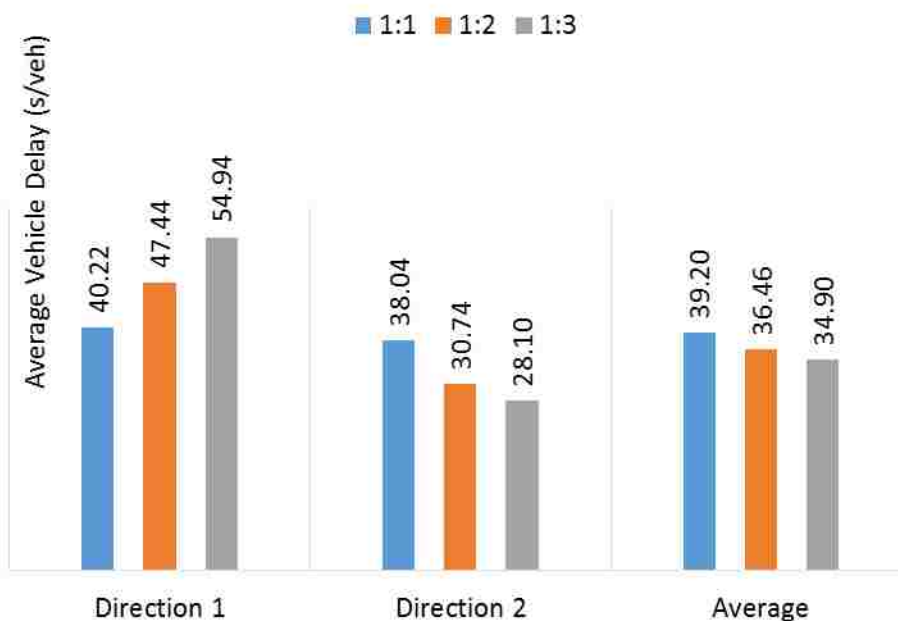

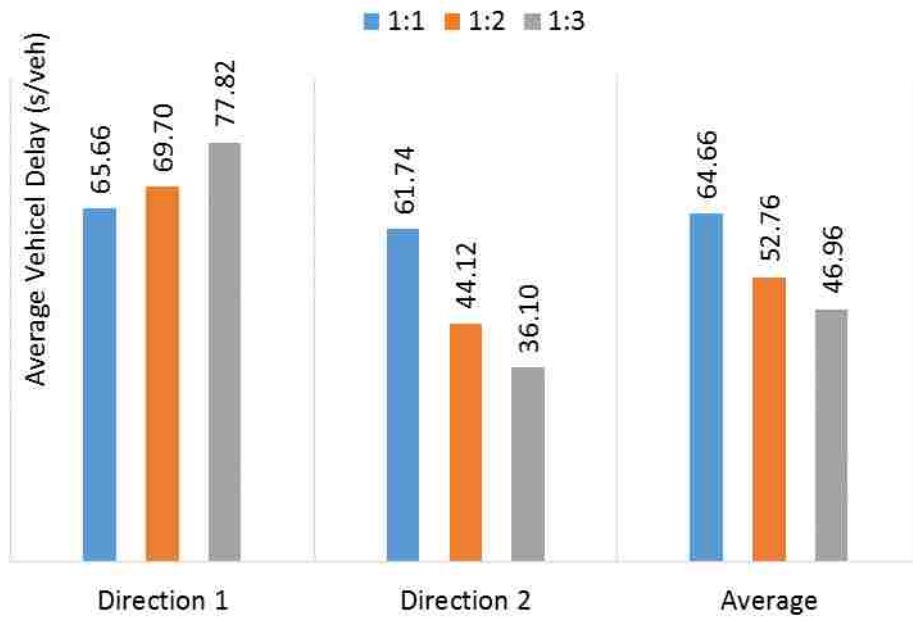**FIGURE 8-2 Vehicle delay for unbalanced traffic flows (moderate traffic)**

73

FIGURE 8-3 Vehicle delay for unbalanced traffic flows (heavy traffic)

Chapter 9   Conclusion

The study first developed a mathematical model to calculate the capacity and vehicle delay for two-lane highway lane-closure work zones. After adjusting the model for the impact of lane closure control plans, it is adequate to make very accurate delay estimations. The mathematical model is more suitable for pre-timed signals where green signal time is fixed for each cycle. Validated by simulation result, the mathematical delay estimation model can be directly applied to find the optimal signal timing while saving the time and effort of running simulations. Simulation models are more powerful in assessing different demand and control scenarios, but microscopic simulations always require a lot of work in calibrations to make them reliable.

The proposed microscopic simulation model uses gap-out distance and max-out green time to approximate the flagger control method in practice. The model output is very close to the field data. Further delay analysis indicates that flagger control is capable to control vehicle delays under low traffic demands. When traffic flow rate increases, flagger control becomes ineffective. Operation cost is another important reason that flagger control is not appropriate for high traffic demands. Real operators cannot check gap-out distance and max-out green time as accurately as the simulation model does, making it impossible to execute flagger method during heavy traffic periods. Thus, fixed time signal control provides a practical alternative solution for some lane closure work zones.

One thing to note in capacity estimation is that directional capacity will change with green time length. We can choose a signal timing plan to achieve a relatively high capacity and also control the vehicle delay at an allowable value. But the total capacity will never exceed directional saturation flow rate.

Unbalanced traffic will result in unbalanced vehicle delay in two directions. Compared to balanced conditions with the same combined traffic rate and total green time,

unbalanced conditions have smaller delay values. But the vehicles travelling in the low-demand bound suffer much longer delay time than vehicles in the high-demand bound. This raises an equity issue. Traffic controllers must consider if it is appropriate to make uneven allocation of the right of way between two directions.

BIBLIOGRAPHY

[1] Transportation Research Board (2010). *Highway capacity manual*. Washington, D.C.

[2] Ceder, A., & Regueros, A. (1990). Traffic control (at alternate one-way sections) during lane closure periods of a two-way highway. In *Proceedings 11th International Symposium on Transportation and Traffic Theory. M. Koshi, Editor. New York: Elsevier Publishing*.

[3] Ceder, A. (1993). Traffic behavior during lane closure periods of a two-lane road. *Transportation and traffic theory*.

[4] Cassidy, M. J., & Han, L. D. (1993). Proposed model for predicting motorist delays at two-lane highway work zones. *Journal of transportation engineering*, *119*(1), 27-42.

[5] Cassidy, M. J., & Han, L. D. (1992). Predicting vehicle delays, and queue lengths on two-lane highways during maintenance activity. In *Proc., TRB 71st Annual Meeting*.

[6] Cassidy, M. J., Son, Y., & Rosowsky, D. V. (1994). Estimating motorist delay at two-lane highway work zones. *Transportation Research Part A: Policy and Practice*, *28*(5), 433-444.

[7] Tae Son, Y. (1999). Queueing delay models for two-lane highway work zones. *Transportation Research Part B: Methodological*, *33*(7), 459-471.

[8] Schonfeld, P., & Chien, S. (1999). Optimal work zone lengths for two-lane highways. *Journal of Transportation Engineering*, *125*(1), 21-29.

[9] Chien, S., Tang, Y., & Schonfeld, P. (2002). Optimizing work zones for two-lane highway maintenance projects. *Journal of Transportation Engineering*, *128*(2), 145-155.

[10] Ceder, A. (2000). An application of an optimal traffic control during lane closure periods of a two-lane road. *Journal of advanced transportation*, *34*(2), 173-190.

[11] Curtis, D. (2001). QuickZone. *Public Roads*, 65(1).

[12] Curtis, D. (2005). Upgrade for the digital work zone: QuickZone now handles more complex projects and more performance measures. *Roads & Bridges*, *43*(6).

[13] Washburn, Scott S., Thomas Hiles, and Kevin Heaslip. (2008). *Impact of Lane Closures on Roadway Capacity: Development of a Two-Lane Work Zone Lane Closure Analysis Procedure (Part A)*. Research Report TRC-FDOT-59056-a-2008 for Transportation Research Center, University of Florida.

[14] Washburn, Scott S., and Carlos O. Cruz-Casas. (2007). *Impact of Trucks on Arterial LOS and Freeway Work Zone Capacity (Part A)* (No. TRC-FDOT-54954-a-2007).

[15] Elefteriadou, L., Arguea, D., Kondyli, A., & Heaslip, K. (2007). *Impact of Trucks on Arterial LOS and Freeway Work Zone Capacity (Part B)* (No. TRC-FDOT-54954-b-2007).

[16] DoT, U. S. (2003). Manual on uniform traffic control devices (MUTCD). *Federal Highway Administration, Washington, DC*.

[17] DeGuzman W.C., et al. (2004) Lane Closure Analysis. *Colorado Dept of Transportation*, Denver, CO.

[18] Cheng, Y., Parker, S. T., Ran, B., & Noyce, D. A. (2015). Integrating Crash, Real-time Traffic, and Lane Closure Data for Statewide Highway Work Zone Safety Analysis. In *Transportation Research Board 94th Annual Meeting* (No. 15-3670).

[19] Rakha H. and Lucic I. (2002). Variable Power Vehicle Dynamics Model for Estimating Maximum Truck Acceleration Levels. *Journal of Transportation Engineering*, Vol.128(5), Sept /Oct. pp. 412-419.

[20] Chen, E., & Tarko, A. P. (2014). Modeling safety of highway work zones with random parameters and random effects models. *Analytic methods in accident research*, *1*, 86-95.

[21] Arguea, D.F. (2006). A Simulation Based Approach to Estimate Capacity of a Temporary Freeway Work Zone Lane Closure. *Master Thesis, University of Florida.*

[22] Zhang, G., Yan, S., & Wang, Y. (2009). Simulation-based investigation on high-occupancy toll lane operations for Washington State Route 167. *Journal of Transportation Engineering*, 135(10), 677-686.

[23] Chen, E., & Tarko, A. P. (2014). Modeling safety of highway work zones with random parameters and random effects models. *Analytic methods in accident research*, *1*, 86-95.

[24] Rouphail, N. M., Courage, K. G., & Strong, D. W. (2006). New Calculation Method for Existing and Extended Highway Capacity Manual Delay Estimation Procedures. In *Transportation Research Board 85th Annual Meeting* (No. 06-0106).

[25] Pline, J. (ed.). Traffic Control Devices Handbook. *Institute of Transportation Engineers, Washington, D.C.*, 2001.

[26] Strong, D. W., & Rouphail, N. M. (2006). Incorporating effects of traffic signal progression into proposed incremental queue accumulation method. In*Transportation Research Board 85th Annual Meeting* (No. 06-0107).

[27] Debnath, A. K., Blackman, R. A., & Haworth, N. L. (2014). Effectiveness of pilot car operations in reducing speeds in a long-term rural highway work zone. In *Proceedings of the 93rd Annual Meeting of the Transportation Research Board*. Transportation Research Board.

[28] Watson Jr, D. C., Hiles, T. W., & Washburn, S. S. (2015). Analysis Methodology for Two-Lane Highways with a Lane Closure. In *Transportation Research Board 94th Annual Meeting* (No. 15-1186).

[29] Chung, Y., Kim, H., & Park, M. (2012). Quantifying non-recurrent traffic congestion caused by freeway work zones using archived work zone and ITS traffic data. *Transportmetrica*, *8*(4), 307-320.

[30] Dion, F., Rakha, H., & Kang, Y. S. (2004). Comparison of delay estimates at under-saturated and over-saturated pre-timed signalized intersections. *Transportation Research Part B: Methodological*, *38*(2), 99-122.

[31] Shibuya, S., Nakatsuji, T., Fujiwara, T., & Matsuyama, E. (1996). Traffic control at flagger-operated work zones on two-lane roads. *Transportation Research Record: Journal of the Transportation Research Board*, *1529*(1), 3-9.

[32] Ak çelik, R., & Rouphail, N. M. (1993). Estimation of delays at traffic signals for variable demand conditions. *Transportation Research Part B: Methodological*, *27*(2), 109-131.

APPENDIX

Site Photos and Data Processing Results

FIGURE A-1 Location and site photos for work zone #1

TABLE A-1 Data processing result for work zone #1

A. Work zone configuration	Value	Unit
AADT	3200	veh/day
Video recording start time	07:03 AM 06/07/13	HH: MM: SS MM/DD/YY
Video recording end time	09:29 AM 06/07/13	HH: MM: SS MM/DD/YY
Work zone subject street name	SR 278	-
Work zone length	1572	ft
Length of shifting/transition area (Side A)	-	ft
Length of Shifting/transition area (Side B)	-	ft
Presence of raised curb on outside edge of street	No	Yes/No
Light condition in work zone area for the non-closed lane	Day	Day/Night
Construction intensity	One lane	Traffic Interruption for both lanes/one lane
B. Traffic control method		
Traffic control method	Flagger	Flagger/signal or others
Cycle length	Not fixed	s
Green time for blocked lane	-	s
Green time for un-blocked lane	-	s
Work zone area speed limit	Slow	mi/h
Posted speed limit for non-work zone area	55	mi/h
C. Roadway geometry		
Lane width (two directions)	12	ft
Shoulder width for the non-closure lane	4	ft
Number of intersections in between work zone area	0	Number
D1. Statistic result – blocked lane		

Flow	-		99.1	veh/h/ln
Truck proportion	-		5/93	%
Queue length	Average		3.2	veh
	Maximum		9	veh
	Minimum		1	veh
Lange changing time	Average		3.32	s
	Maximum		10.0	s
	Minimum		2.0	s
Work zone travel time	Average		38.60	s
	Maximum		46.0	s
	Minimum		25.0	s
Work zone travel speed	Average		28.08	mi/h
	Maximum		42.87	mi/h
	Minimum		17.86	mi/h

D2. Statistic result – unblocked lane

Flow	-		76.3	veh/h/ln
Truck proportion	-		14/63	%
Queue length	Average		2.7	veh
	Maximum		4	veh
	Minimum		1	veh
Work zone travel time	Average		33.22	s
	Maximum		52.0	s
	Minimum		18.0	s
Work zone travel speed	Average		33.27	mi/h
	Maximum		59.54	mi/h
	Minimum		20.61	mi/h

Observations and comments

- Morning peak was not observed.

- The average queue length was one vehicle, and the maximum queue length was 8 vehicles.

- The lane shifting area was not clear, and the lane markings did not cover the entire work zone area.

- Some drivers in the blocked lane would not change their driving lanes right after the flaggers. They would choose to drive in the middle of the road for a while and finish the lane shifting before they arrive at the working area.

FIGURE A-2 Location and site photos for work zone #2

TABLE A-2 Data processing result for work zone #2

A. Work zone configuration		Value	Unit
AADT		3200	veh/day
Video recording start time		04:00 PM 06/07/13	HH: MM: SS MM/DD/YY
Video recording end time		05:00 PM 06/07/13	HH: MM: SS MM/DD/YY
Work zone subject street name		SR 278	-
Work zone length		2100	ft
Length of shifting/transition area (Side A)		-	ft
Length of Shifting/transition area (Side B)		-	ft
Presence of raised curb on outside edge of street		No	Yes/No
Light condition in work zone area for the non-closed lane		Day	Day/Night
Construction intensity		One lane	Traffic Interruption for both lanes/one lane
B. Traffic control method			
Traffic control method		Flagger	Flagger/signal or others
Cycle length		Not fixed	s
Green time for blocked lane		-	s
Green time for un-blocked lane		-	s
Work zone area speed limit		Slow	mi/h
Posted speed limit for non-work zone area		55	mi/h
C. Roadway geometry			
Lane width (two directions)		12	ft
Shoulder width for the non-closure lane		-	ft
Number of intersections in between work zone area		0	Number
D1. Statistic result – blocked lane			
Flow	-	99.1	veh/h/ln
Truck proportion	-	5/93	%
Queue length	Average	-	veh
	Maximum	-	veh
	Minimum	-	veh
Lange changing time	Average	-	s
	Maximum	-	s
	Minimum	-	s

Work zone travel time	Average		-	s
	Maximum		-	s
	Minimum		-	s
Work zone travel speed	Average		-	mi/h
	Maximum		-	mi/h
	Minimum		-	mi/h
D2. Statistic result – unblocked lane				
Flow	**-**		76.3	veh/h/ln
Truck proportion	**-**		14/63	%
Queue length	Average		-	veh
	Maximum		-	veh
	Minimum		-	veh
Work zone travel time	Average		-	s
	Maximum		-	s
	Minimum		-	s
Work zone travel speed	Average		-	mi/h
	Maximum		-	mi/h
	Minimum		-	mi/h

Note: data is incomplete due to camera failure

Observations and comments

- Evening peak was observed.

- The average queue length was longer than that in the morning.

- The lane shifting area was not clear, and the lane markings did not cover the entire work zone area.

- Because the markings did not cover the entire work zone area, some drivers in the blocked lane would not change their driving lanes right after the flaggers. They would choose to drive in the middle of the road for a while and finish the lane shifting before they arrive at the actual working area.
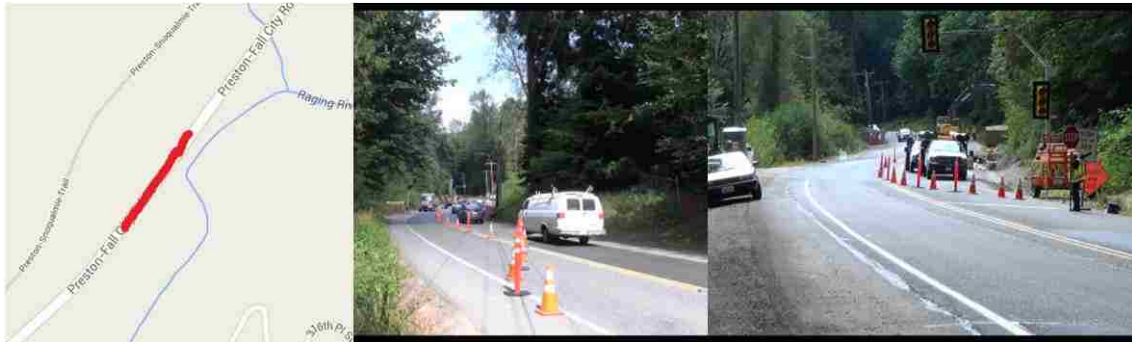
FIGURE A-3 Location and site photos for work zone #3

TABLE A-3 Data processing result for work zone #3

A. Work zone configuration		Value	Unit
AADT		7938	veh/day
Video recording start time		02:30 PM 07/29/13	HH: MM: SS MM/DD/YY
Video recording end time		03:15 PM 07/29/13	HH: MM: SS MM/DD/YY
Work zone subject street name		Preston-Fall City Road	-
Work zone length		800	ft
Length of shifting/transition area (Side A)		168	ft
Length of Shifting/transition area (Side B)		70	ft
Presence of raised curb on outside edge of street		No	Yes/No
Light condition in work zone area for the non-closed lane		Day	Day/Night
Construction intensity		One lane	Traffic Interruption for both lanes/one lane
B. Traffic control method			
Traffic control method		Flagger	Flagger/signal or others
Cycle length		Not fixed	s
Green time for blocked lane		-	s
Green time for un-blocked lane		-	s
Work zone area speed limit		Slow	mi/h
Posted speed limit for non-work zone area		55	mi/h
C. Roadway geometry			
Lane width (two directions)		12	ft
Shoulder width for the non-closure lane		3-4	ft
Number of intersections in between work zone area		0	Number
D1. Statistic result – blocked lane			
Flow	-	261	veh/h/ln
Truck proportion	-	12/238	%
Queue length	Average	8.0	veh
	Maximum	12	veh
	Minimum	2	veh
Lange changing time	Average	2.99	s

	Maximum	5.0	s
	Minimum	1.0	s
Work zone travel time	Average	25.94	s
	Maximum	49.0	s
	Minimum	11.0	s
Work zone travel speed	Average	22.52	mi/h
	Maximum	49.58	mi/h
	Minimum	11.13	mi/h

D2. Statistic result – unblocked lane

Flow	-	328	veh/h/ln
Truck proportion	-	26/299	%
Queue length	Average	6.5	veh
	Maximum	12	veh
	Minimum	2	veh
Work zone travel time	Average	22.02	s
	Maximum	40.0	s
	Minimum	10.0	s
Work zone travel speed	Average	25.77	mi/h
	Maximum	54.54	mi/h
	Minimum	13.64	mi/h

Observations and comments

- High traffic volume was observed, most arrival intervals are within 30 seconds.

- The lane shifting area was clear, and the lane markings covered the entire work zone area.

- The flagger would not change until the queue for one direction is discharged.

- Some drivers would stop their vehicles far from the flaggers. The distance could be as far as 3 meters (10 ft).

FIGURE A-4 Location and site photos for work zone #4

TABLE A-4 Data processing result for work zone #4

A. Work zone configuration		Value	Unit
AADT		7938	veh/day
Video recording start time		03:15 PM 07/29/13	HH: MM: SS MM/DD/YY
Video recording end time		05:00 PM 07/29/13	HH: MM: SS MM/DD/YY
Work zone subject street name		Preston-Fall City Road	-
Work zone length		800	ft
Length of shifting/transition area (Side A)		168	ft
Length of Shifting/transition area (Side B)		70	ft
Presence of raised curb on outside edge of street		No	Yes/No
Light condition in work zone area for the non-closed lane		Day	Day/Night
Construction intensity		One lane	Traffic Interruption for both lanes/one lane
B. Traffic control method			
Traffic control method		Signal	Flagger/signal or others
Cycle length		145	s
Green time		40	s
Yellow time (between green and red)		8	s
Work zone area speed limit		Slow	mi/h
Posted speed limit for non-work zone area		45	mi/h
C. Roadway geometry			
Lane width (two directions)		12	ft
Shoulder width for the non-closure lane		3-4	ft
Number of intersections in between work zone area		0	Number
D1. Statistic result – blocked lane			
Flow	-	261	veh/h/ln
Truck proportion	-	12/238	%
Queue length	Average	7.6	veh
	Maximum	15	veh
	Minimum	1	veh
Lange changing time	Average	2.43	s
	Maximum	8.0	s
	Minimum	1.0	s
Work zone travel time	Average	26.96	s
	Maximum	49.0	s
	Minimum	11.0	s
Work zone travel speed	Average	21.83	mi/h
	Maximum	49.59	mi/h
	Minimum	11.13	mi/h
D2. Statistic result – unblocked lane			
Flow	-	328	veh/h/ln

Truck proportion	**-**		26/299	%
Queue length	Average		8.5	veh
	Maximum		15	veh
	Minimum		1	veh
Work zone travel time	Average		21.21	s
	Maximum		40.0	s
	Minimum		7.0	s
Work zone travel speed	Average		26.78	mi/h
	Maximum		77.92	mi/h
	Minimum		13.64	mi/h

Observations and comments

- High traffic volume was observed. Over-saturated traffic condition was observed.

- The lane shifting area was clear, and the lane markings covered the entire work zone area.

- The signal control method and flagger control method were used at the same time for about 1 minute.

FIGURE A-5 Location and site photos for work zone #5

TABLE A-5 Data processing result for work zone #5

A. Work zone configuration	Value	Unit
AADT	7424	veh/day
Video recording start time	12:30 PM 08/14/13	HH: MM: SS MM/DD/YY
Video recording end time	01:30 PM 08/14/13	HH: MM: SS MM/DD/YY
Work zone subject street name	Preston-Fall City Road	-
Work zone length	1600	ft
Length of shifting/transition area (Side A)	-	ft
Length of Shifting/transition area (Side B)	-	ft

86

Presence of raised curb on outside edge of street		No	Yes/No
Light condition in work zone area for the non-closed lane		Day	Day/Night
Construction intensity		One lane	Traffic Interruption for both lanes/one lane

B. Traffic control method

Traffic control method		Flagger	Flagger/signal or others
Cycle length		Not fixed	s
Green time for blocked lane		-	s
Green time for un-blocked lane		-	s
Work zone area speed limit		Slow	mi/h
Posted speed limit for non-work zone area		45	mi/h

C. Roadway geometry

Lane width (two directions)		12	ft
Shoulder width for the non-closure lane		3-4	ft
Number of intersections in between work zone area		2	Number

D1. Statistic result – blocked lane

Flow	-	185.8	veh/h/ln
Truck proportion	-	9/188	%
Queue length	Average	9.4	veh
	Maximum	29	veh
	Minimum	2	veh
Lange changing time	Average	2.04	s
	Maximum	1.0	s
	Minimum	1.0	s
Work zone travel time	Average	68.76	s
	Maximum	98.0	s
	Minimum	48.0	s
Work zone travel speed	Average	16.28	mi/h
	Maximum	22.73	mi/h
	Minimum	11.13	mi/h

D2. Statistic result – unblocked lane

Flow	-	149.9	veh/h/ln
Truck proportion	-	9/158	%
Queue length	Average	9.6	veh
	Maximum	16	veh
	Minimum	3	veh
Work zone travel time	Average	58.92	s
	Maximum	77.0	s
	Minimum	27.0	s
Work zone travel speed	Average	18.83	mi/h
	Maximum	40.40	mi/h
	Minimum	14.17	mi/h

Observations and comments

- High traffic volume was observed.

- The lane shifting area was clear, and the lane markings covered the entire work zone area.

- Though there were two intersections in between work zone area, traffic counts from the intersections were not observed.

FIGURE A-6 Location and site photos for work zone #6

TABLE A-6 Data processing result for work zone #6

A. Work zone configuration	Value	Unit
AADT	7424	veh/day
Video recording start time	02:15 PM 08/14/13	HH: MM: SS MM/DD/YY
Video recording end time	03:15 PM 08/14/13	HH: MM: SS MM/DD/YY
Work zone subject street name	Preston-Fall City Road	-
Work zone length	1-2 miles (moving)	-
Length of shifting/transition area (Side A)	-	ft
Length of Shifting/transition area (Side B)	-	ft
Presence of raised curb on outside edge of street	No	Yes/No
Light condition in work zone area for the non-closed lane	Day	Day/Night
Construction intensity	One lane	Traffic Interruption for both lanes/one lane
B. Traffic control method		
Traffic control method	Pilot car	Flagger/signal or others
Cycle length	Not fixed	s
Green time for blocked lane	-	s
Green time for un-blocked lane	-	s
Work zone area speed limit	Slow	mi/h
Posted speed limit for non-work zone area	45	mi/h
C. Roadway geometry		
Lane width (two directions)	-	ft
Shoulder width for the non-closure lane	3-4	ft

Number of intersections in between work zone area		0	Number
D1. Statistic result – blocked lane			
Flow	-	212.7	veh/h/ln
Truck proportion	-	2/112	%
Queue length	Average	-	veh
	Maximum	-	veh
	Minimum	-	veh
Lange changing time	Average	2.16	s
	Maximum	5.0	s
	Minimum	1.0	s
Work zone travel time	Average	-	s
	Maximum	-	s
	Minimum	-	s
Work zone travel speed	Average	-	mi/h
	Maximum	-	mi/h
	Minimum	-	mi/h
D2. Statistic result – unblocked lane			
Flow	-	206.1	veh/h/ln
Truck proportion	-	13/197	%
Queue length	Average	15.67	veh
	Maximum	22	veh
	Minimum	7	veh
Work zone travel time	Average	-	s
	Maximum	-	s
	Minimum	-	s
Work zone travel speed	Average	-	mi/h
	Maximum	-	mi/h
	Minimum	-	mi/h

Observations and comments

- Moving project.

- Work zone length varies from 1~2 miles during data collection period.

- High traffic volume was observed. The traffic was over-saturated during the entire

observation period.

- The lane shifting area was clear, and the lane markings covered the entire work zone

area.

- Pilot car control method was observed from this work zone. However, as the flagger moved very frequently at one work zone end, only flow and arrival rate from the fixed end were observed from this site.

- For the road side videos, the cameras were unable to record the queue length because the queue was too long.

Vehicle Arrival Patterns

Work Zone #1 Complete data was collected and processed. As direction 2 has a very low demand, very few vehicles were observed. Vehicle headway distribution is highly disperse.
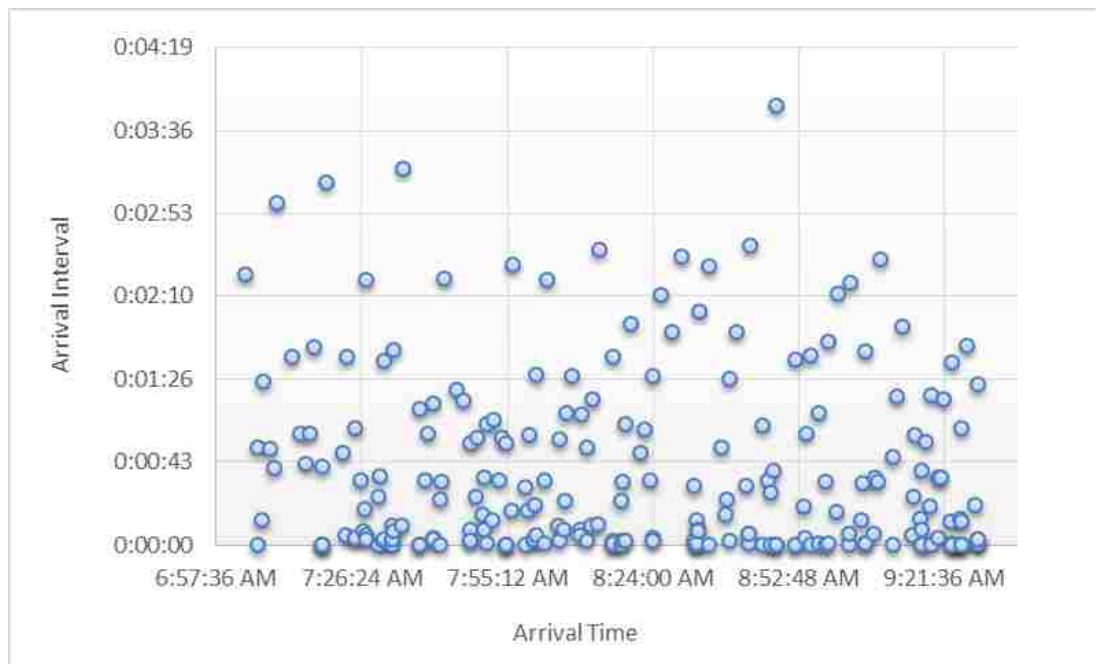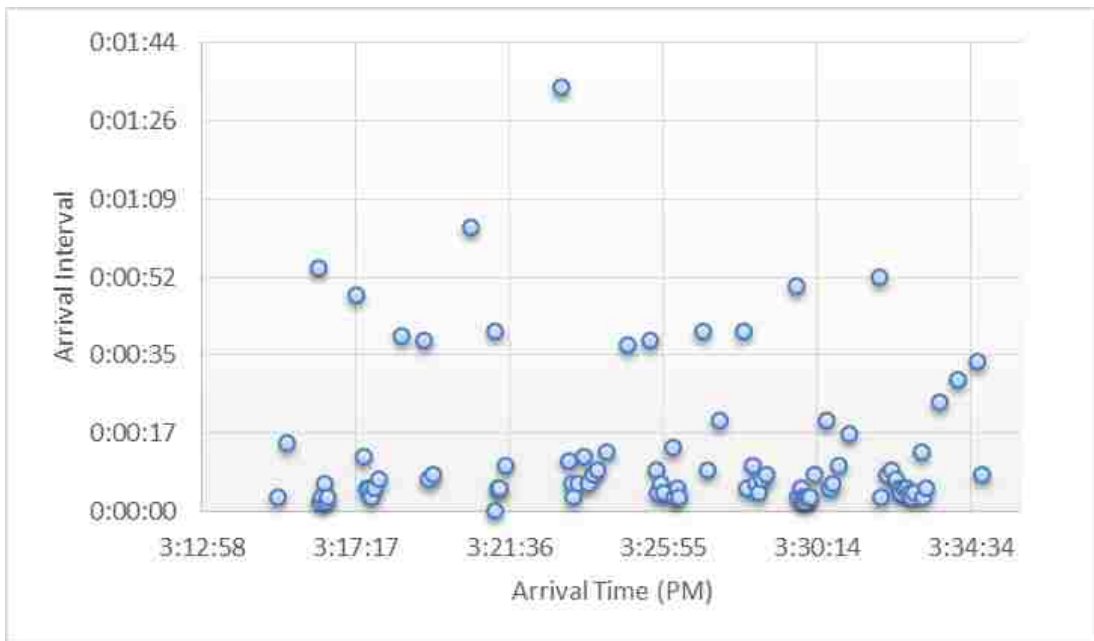

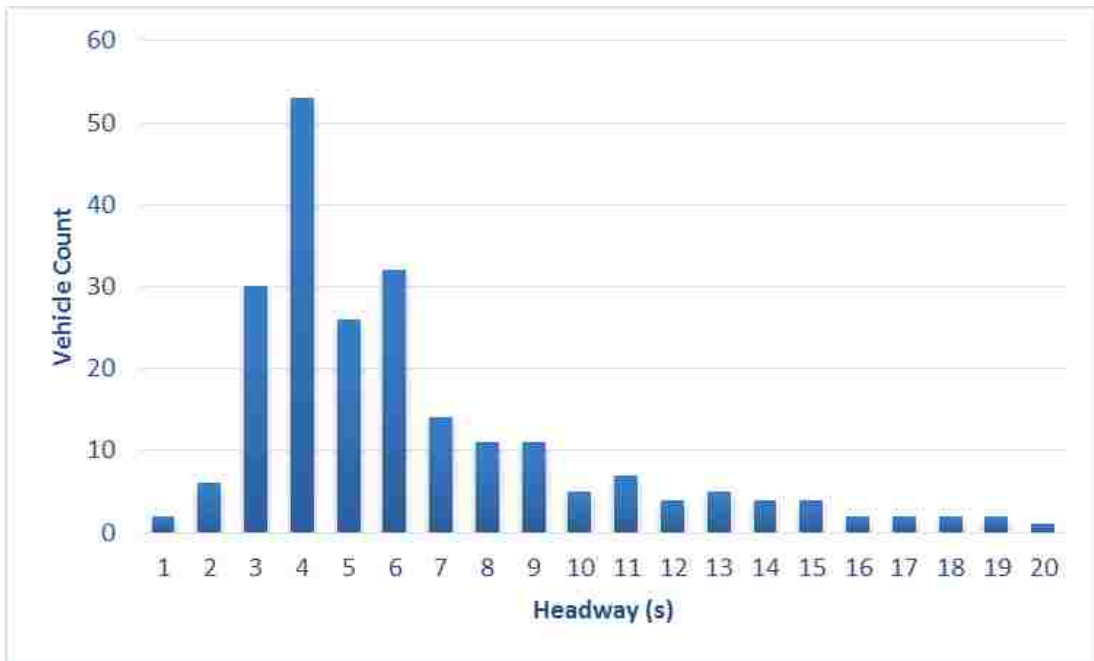**FIGURE A-7 Arrival pattern for work zone #1 direction 1 (blocked lane)**
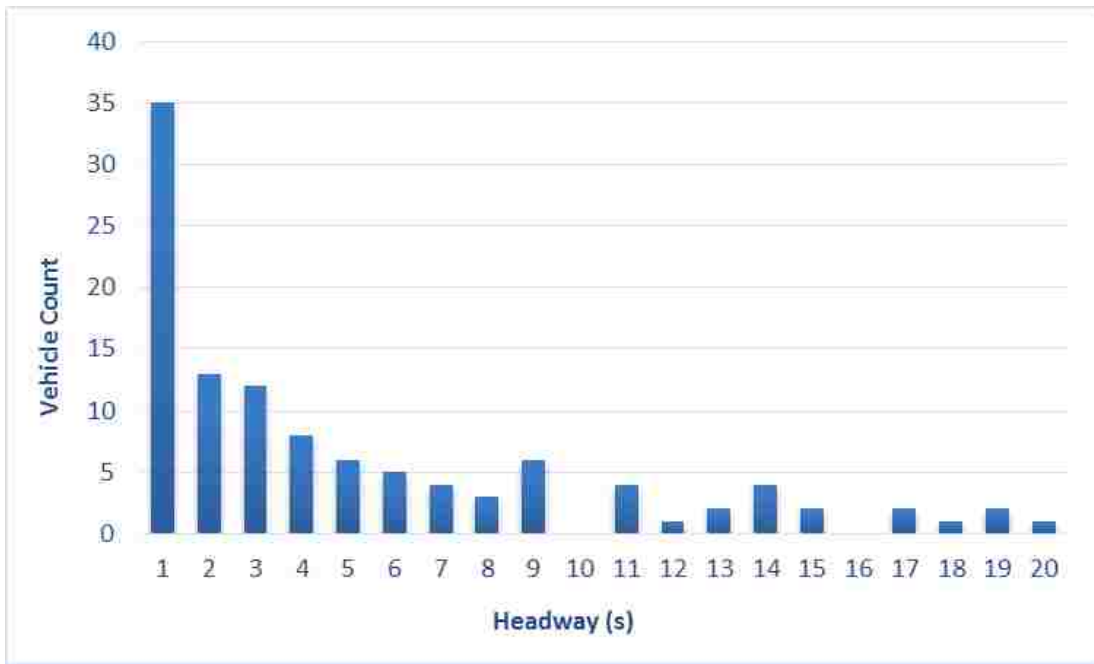
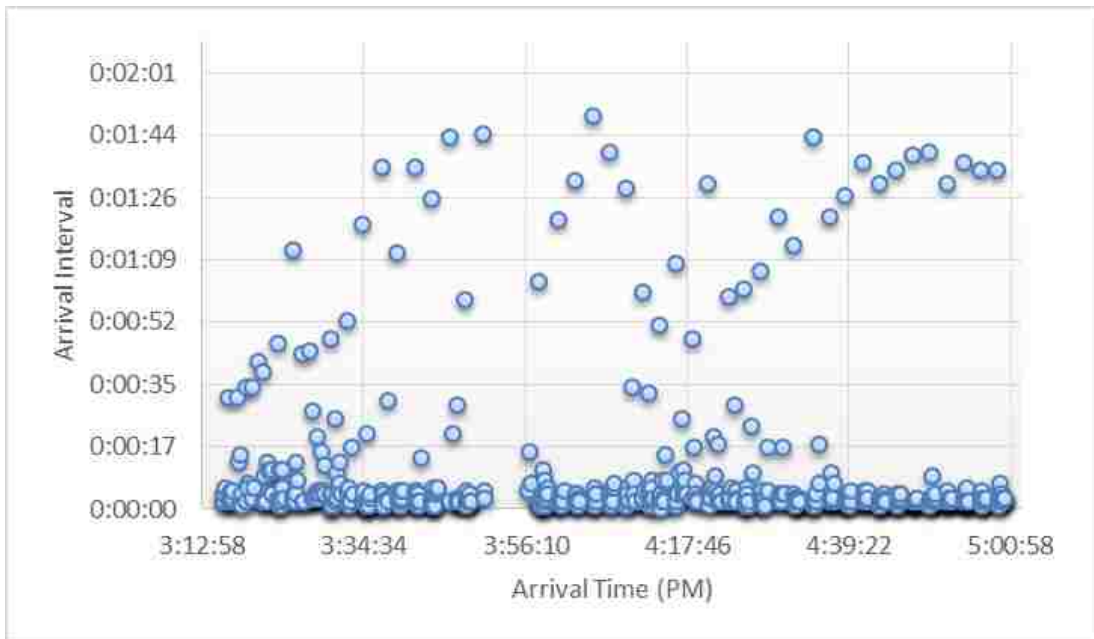**FIGURE A-8 Headway distribution for work zone #1 direction 1 (blocked lane)**
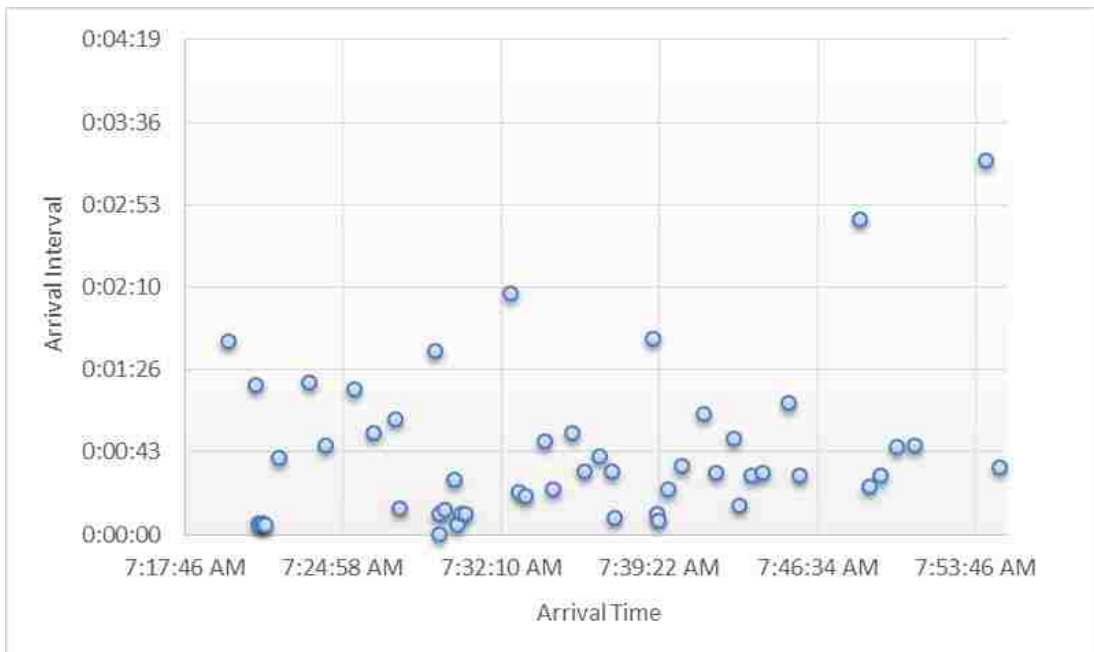
FIGURE A-9 Arrival pattern for work zone #1 direction 2 (unblocked lane)
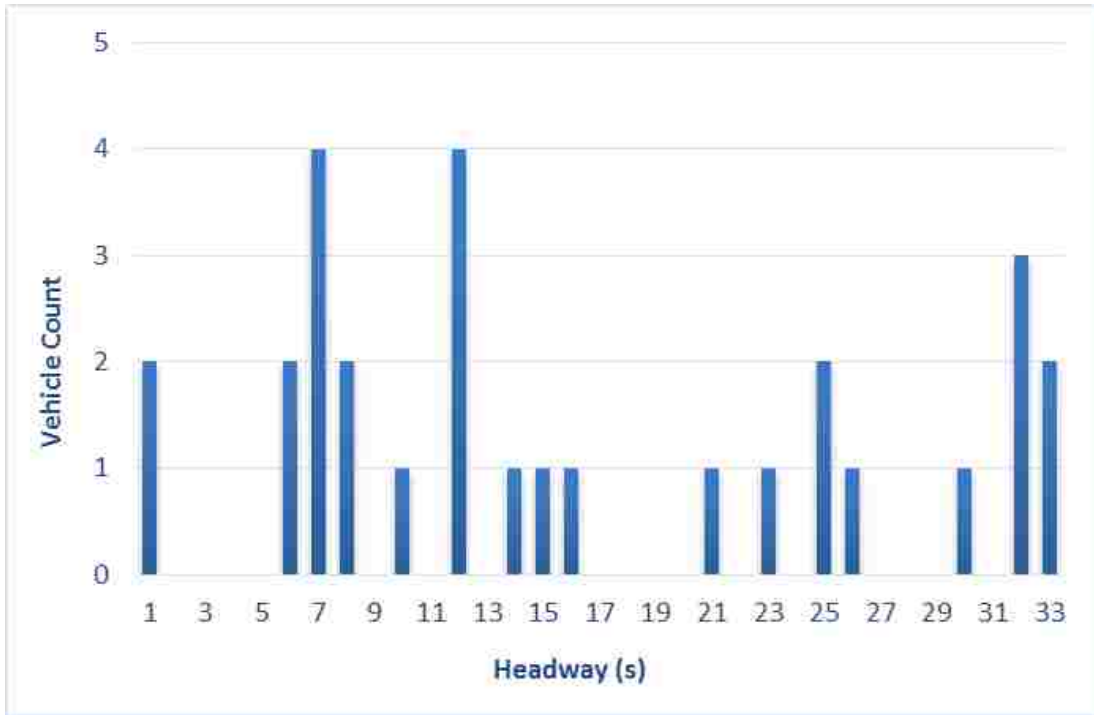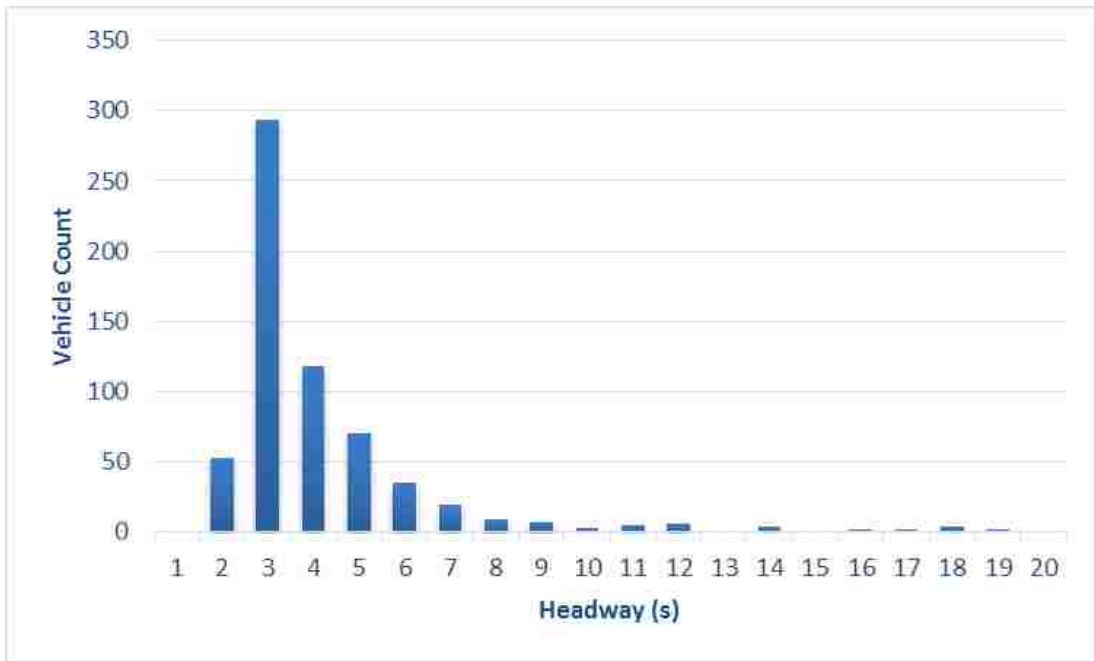
FIGURE A-10 Headway distribution for work zone #1 direction 2 (unblocked lane)

Work Zone #2 Data for the unblocked lane is incomplete because of camera failure.
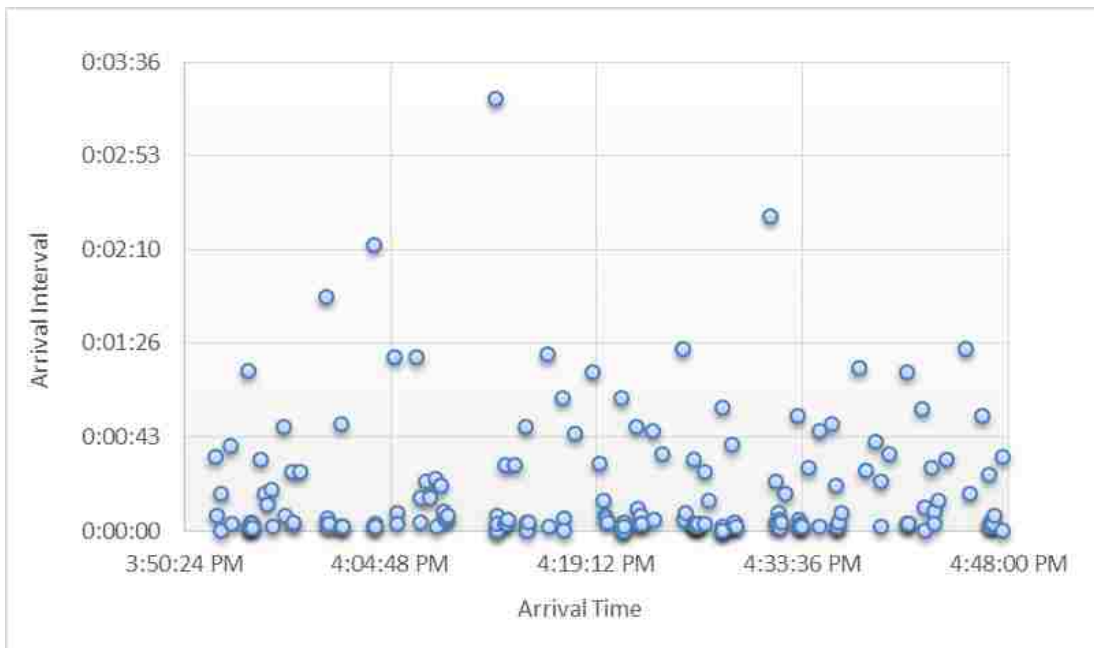
FIGURE A-11 Arrival pattern for work zone #2 direction 2 (unblocked lane)
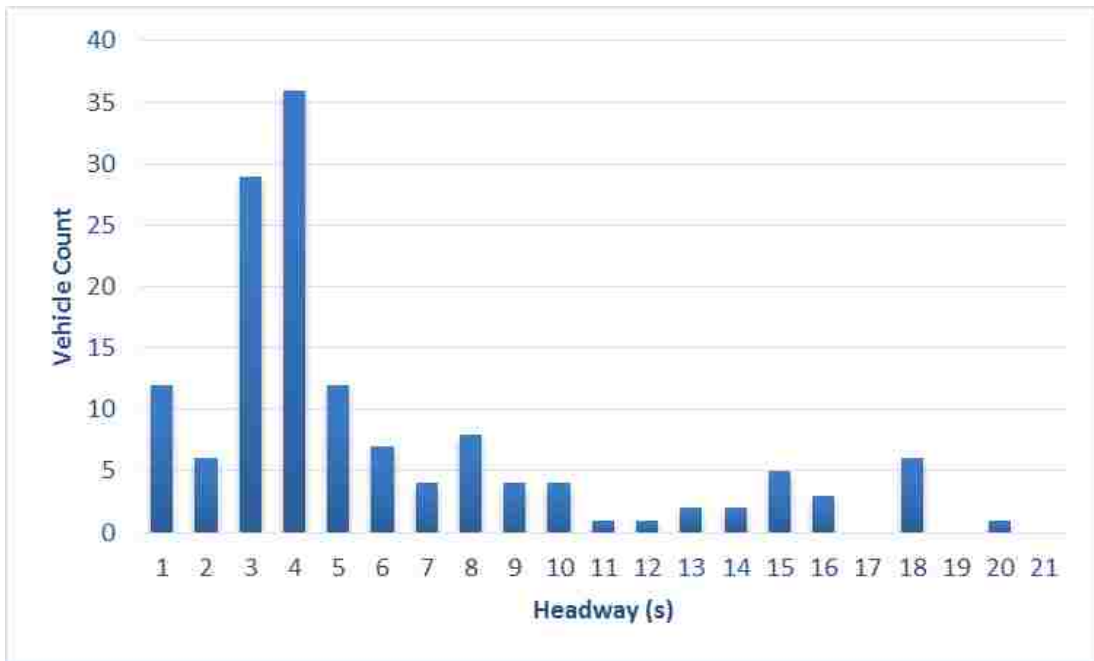
FIGURE A-12 Headway distribution for work zone #2 direction 2 (unblocked lane)

Work Zone #3 Complete data was collected and processed.
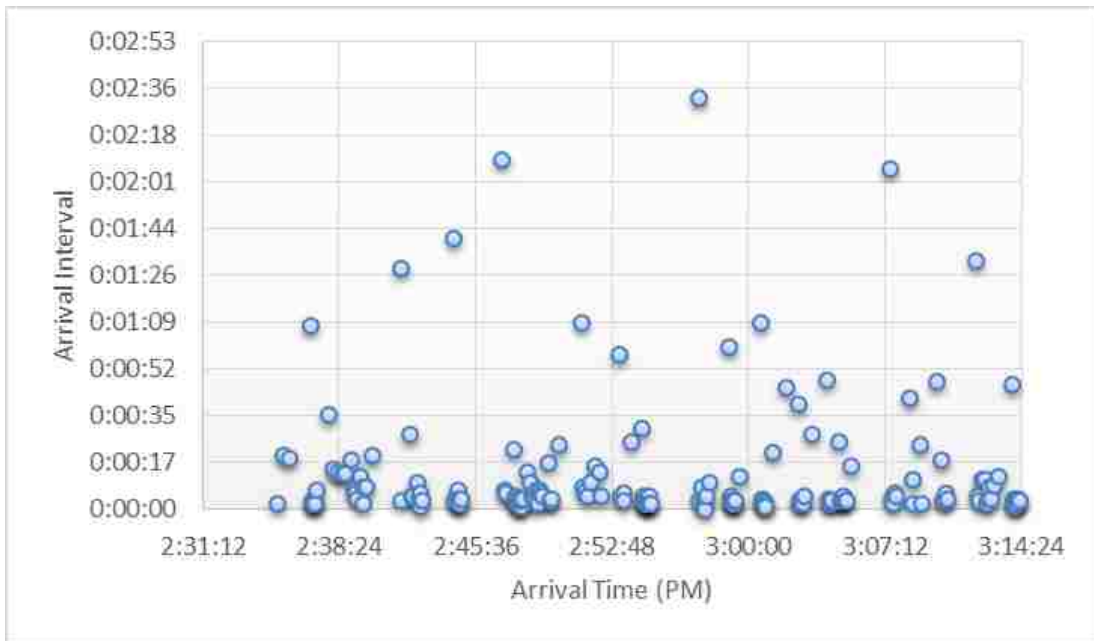
FIGURE A-13 Arrival pattern for work zone #3 direction 1 (blocked lane)
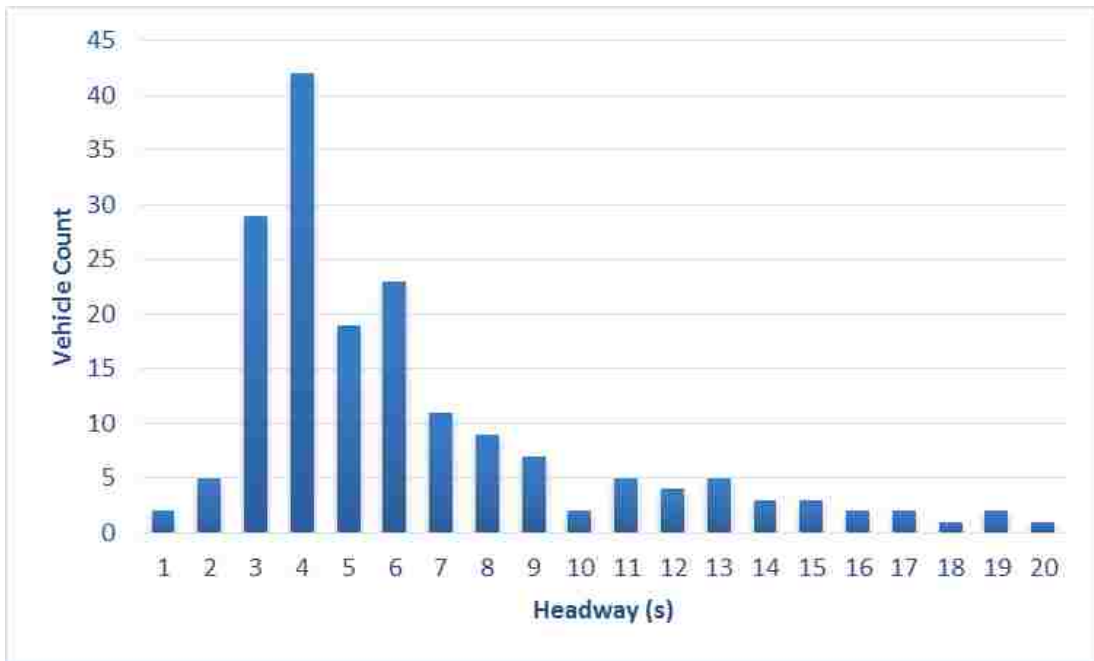
FIGURE A-14 Headway distribution for work zone #3 direction 1 (blocked lane)
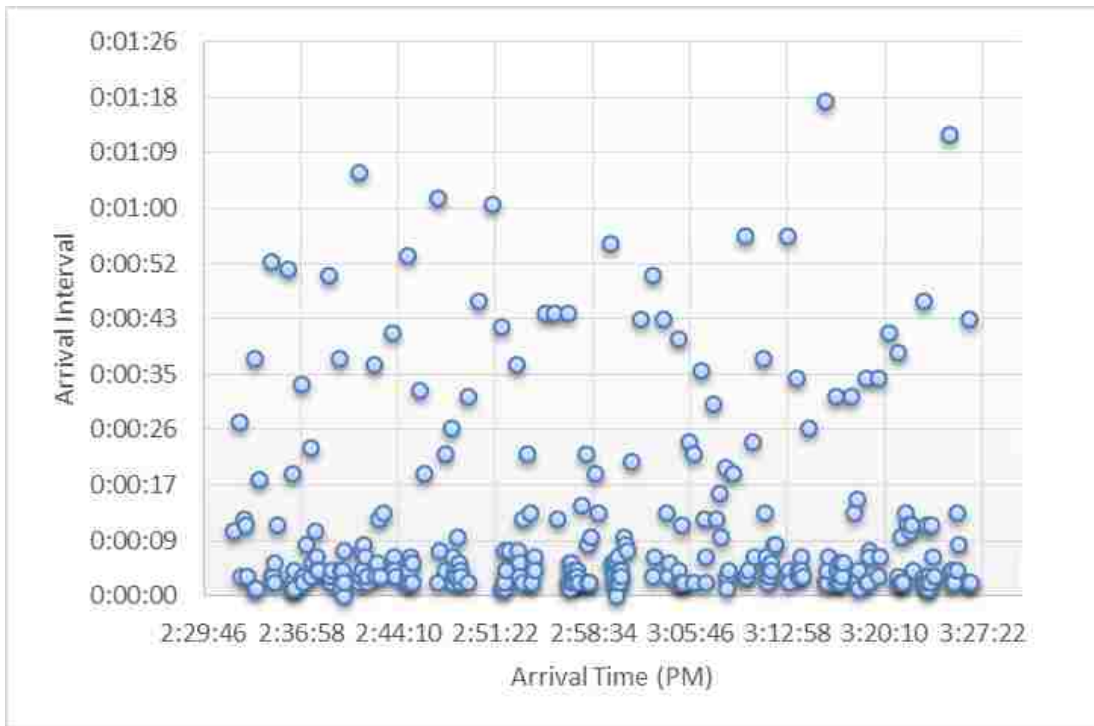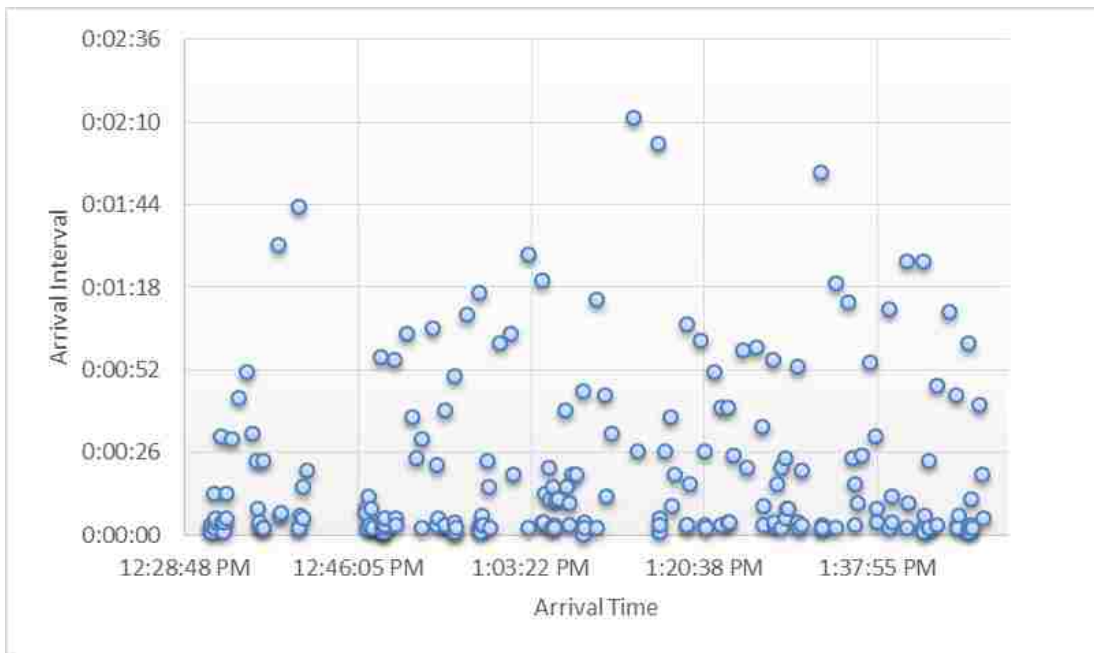

FIGURE A-15 Arrival pattern for work zone #3 direction 2 (unblocked lane)
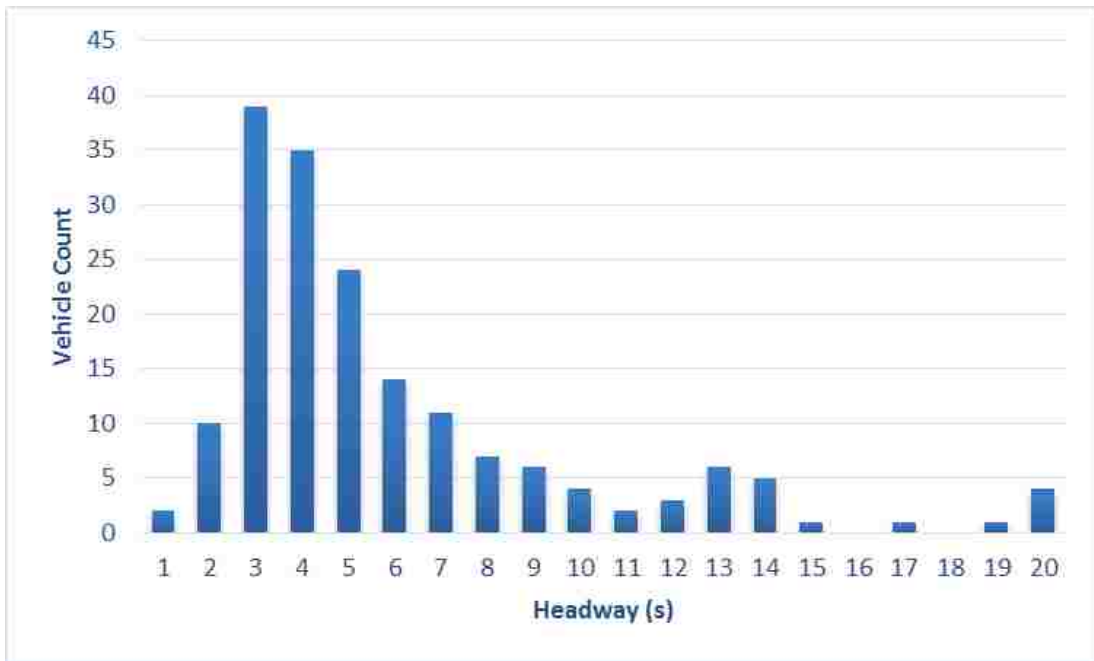
FIGURE A-16 Headway distribution for work zone #3 direction 2 (unblocked lane)

Work Zone #4 After 3:34:52 PM, camera #1 was block by signal head. For direction 1 vehicles arrived after that time, arrival times were not recorded.

FIGURE A-17 Arrival pattern for work zone #4 direction 1 (blocked lane)
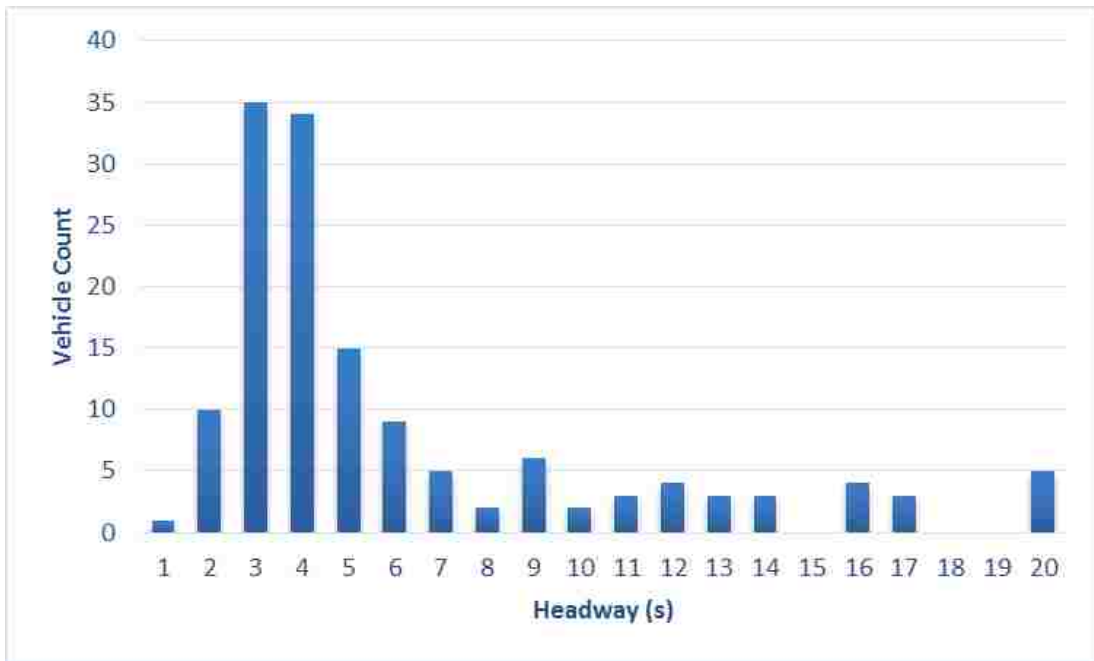
FIGURE A-18 Headway distribution for work zone #4 direction 1 (blocked lane)
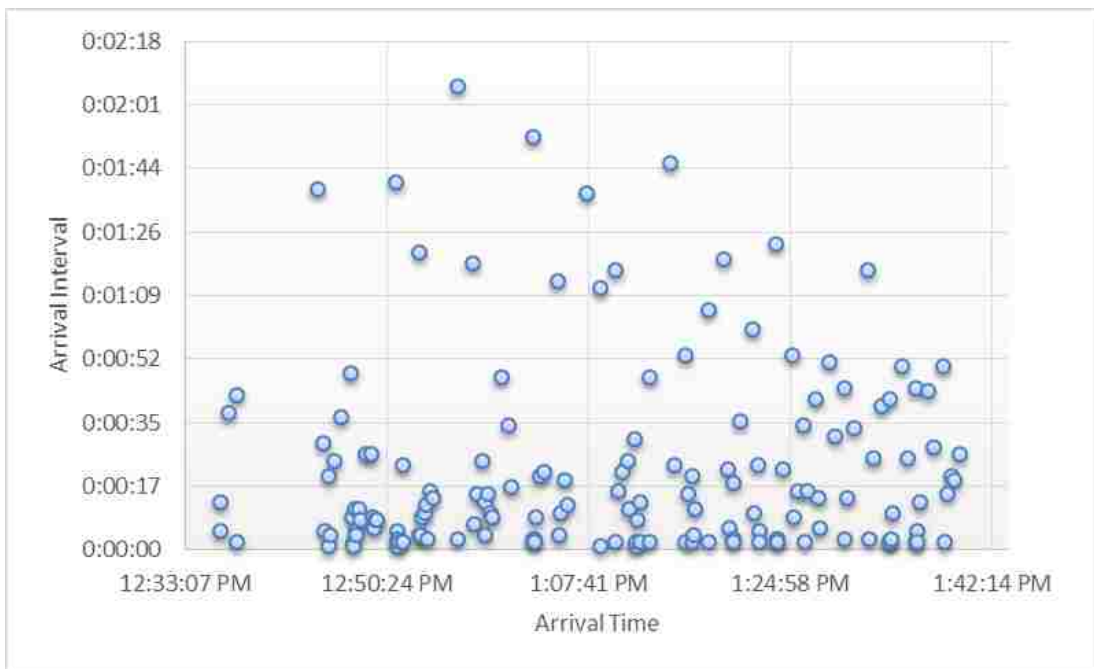

FIGURE A-19 Arrival pattern for work zone #4 direction 2 (unblocked lane)

FIGURE A-20 Headway distribution for work zone #4 direction 2 (unblocked lane)

Work Zone #5 From 12:41:37 PM to 12:46:28 PM, the research team was replacing batteries for video cameras. So two more-than-5-minute arrival intervals were shown in the arrival patterns because of data missing.

FIGURE A-21 Arrival pattern for work zone #5 direction 1 (blocked lane)

97

FIGURE A-22 Headway distribution for work zone #5 direction 1 (blocked lane)

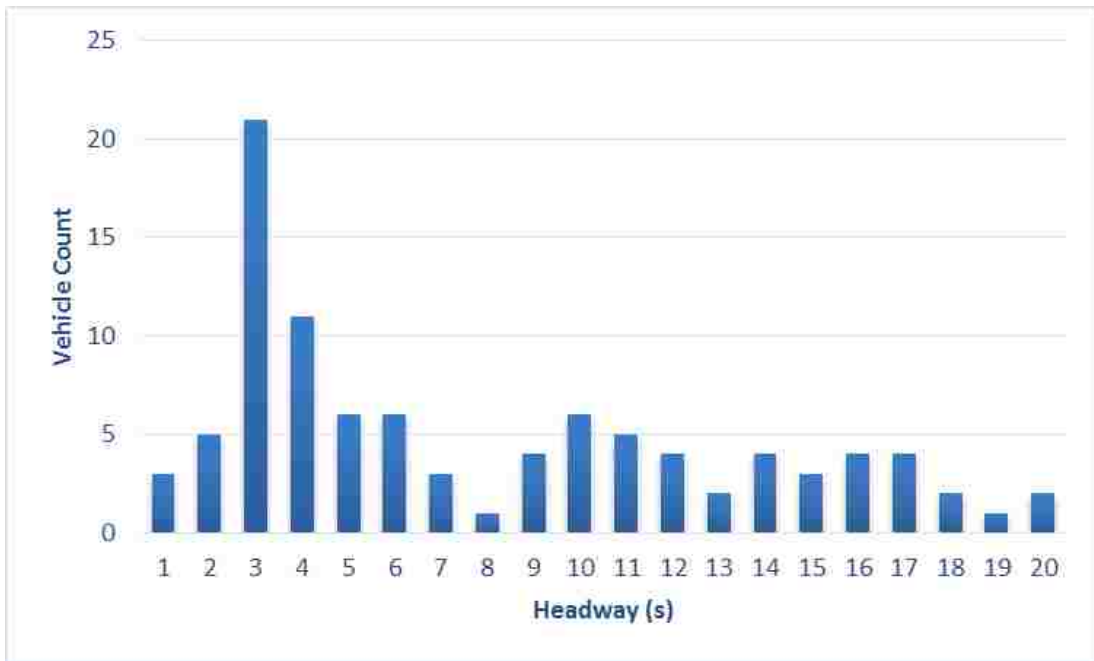**FIGURE A-23 Arrival pattern for work zone #5 direction 2 (unblocked lane)**

FIGURE A-24 Headway distribution for work zone #5 direction 2 (unblocked lane)

Work Zone #6 According to the arrival pattern figure, no vehicle arrival was observed from 2:30:33 PM to 2:41:04 PM. This is because the queue has exceeded the video camera recording range, we were unable to observe new arrivals.
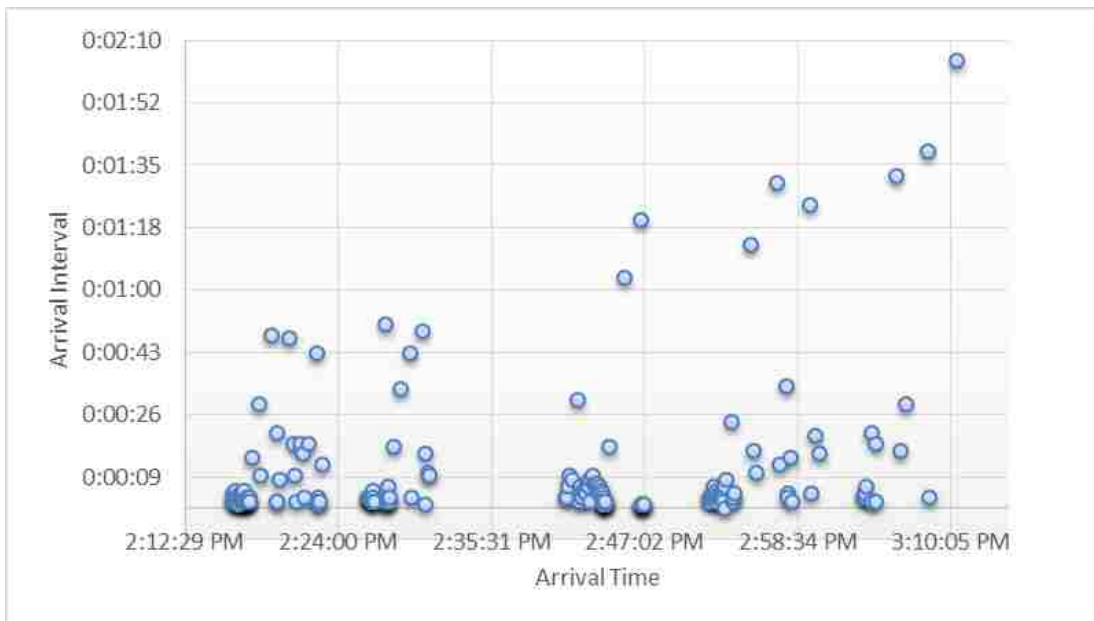

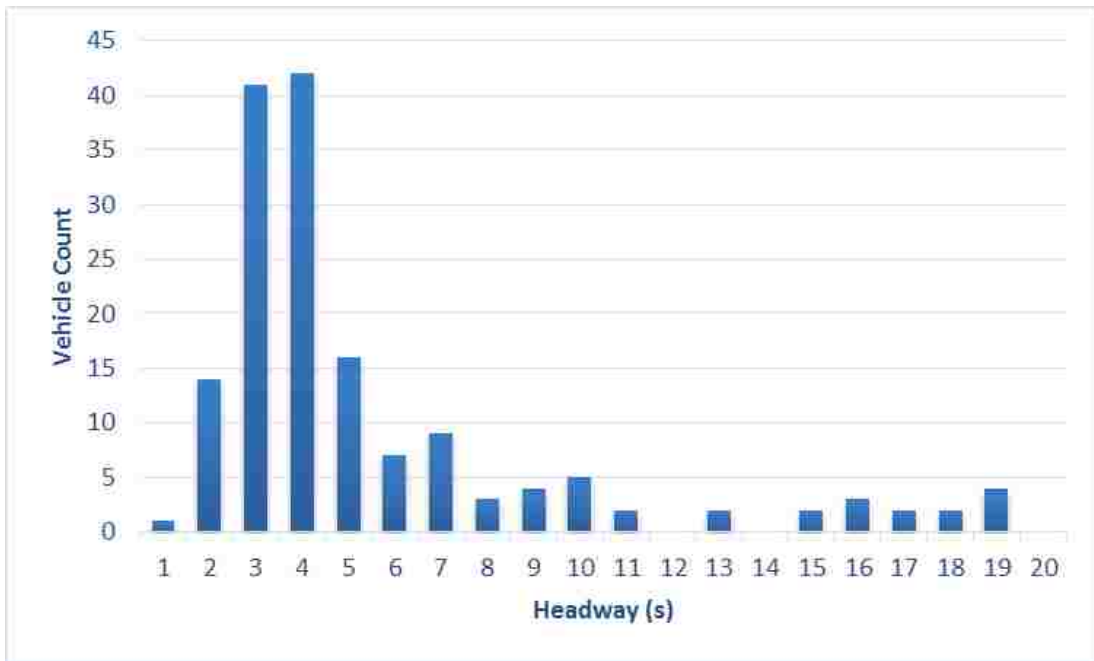**FIGURE A-25 Arrival pattern for work zone #6 direction 2 (unblocked lane)**

FIGURE A-26 Headway distribution for work zone #6 direction 2 (unblocked lane)